Quaternary Science Reviews 318 (2023) 108315

Contents lists available at ScienceDirect

Quaternary Science Reviews

journal homepage: www.elsevier.com/locate/quascirev

Vegetation, fire and climate history in central-western Tasmania (41°S), Australia, over the last ~21,000 years

William I. Henríquez [a,*], Michael-Shawn Fletcher [a,b], Anthony Romano [a]

[a] School of Geography, Earth and Atmospheric Sciences, The University of Melbourne, Carlton, VIC3053, Australia
[b] Indigenous Knowledge Institute, The University of Melbourne, Parkville, VIC3010, Australia

ARTICLE INFO

Keywords:
Southern westerly winds
Centra-western tasmania
Southern middle latitudes
Rainforest
Buttongrass

ABSTRACT

We present high resolution pollen and macroscopic charcoal records from Basin Lake, a relatively small mid-latitude (42°S) lake located in central-western Tasmania, Australia, to examine vegetation, fire and climate change since and during the Last Glacial Maximum (LGM). We find dominance of cold-resistant alpine vegetation with buttongrass moorland and scant trees between ~21.0-17.7 cal kyr BP, with local biomass burning and low lake levels between ~21.0-20.0 cal kyr BP and a reduction in local biomass burning and a rise in lake levels between ~20.0-17.7 cal kyr BP. These data suggest glacial-cold conditions during the last millennia of the LGM, with relatively humid conditions between ~21.0-20.0 cal kyr BP and a further increase in humidity between ~20.0-17.7 cal kyr BP. These shifts suggest an intensification of the South Westerly Winds (SWW) over the site between ~20.0-17.7 cal kyr BP. An increase in cold-temperate rainforest taxa followed between ~17.7-16.0 cal kyr BP along with lake-level lowering, suggesting a warm pulse and southward shift of the SWW at the beginning of the Last Glacial Termination (T1). Subsequent cold-temperate conditions and increased precipitation ensued between ~16.0-14.9 cal kyr BP promoted by increased SWW influence. A rise in cold-resistant and hygrophilous rainforest taxa and lower biomass burning activity occurred between ~14.9-12.8 cal kyr BP under colder conditions, enhanced precipitation and major SWW influence. A multi-millennial warm/dry interval began at ~12.8 cal kyr BP with a decline in rainforest taxa, high fire activity and low lake levels and a further opening of the vegetation in response to elevated biomass burning between ~11.1-8.9 cal kyr BP. We suggest a decline in the SWW influence that started at ~12.8 cal kyr BP and accentuated between ~11.1-8.9 cal kyr BP at the beginning of the Holocene. We detect increases in precipitation between ~8.9-5.8, ~3.4-1.9 cal kyr BP and the last ~900 years, with declines in the intervening intervals. Our data indicate a pronounced and sustained fire-driven shift to a more open and shrub dominant landscape after ~5.0 cal kyr BP, in synchronous with other pollen data from Tasmania's west, reflecting an increased efficacy of Aboriginal burning under more variable and overall reduced precipitation. Our climate inferences from Basin Lake are coherent with variations of the SWW identified in other terrestrial mid-latitudes records, suggesting synchronic changes in the SWW during and since the LGM.

1. Introduction

Deciphering the timing, magnitude and direction of past climate changes since the Last Glacial Maximum (LGM, ~24.0-18.0 cal kyr BP; cal kyr BP = 1000 calendar years before present; present = 1950 CE) has been an important subject in paleoclimate studies from the middle latitudes of the Southern Hemisphere (e.g. Fletcher et al., 2021a; Moreno et al., 2018; Newnham et al., 2007). This broad region is under the permanent influence of the Southern Westerly Winds (SWW), a zonally symmetric component of the global atmospheric system that govern the climate of southern mid-latitudes landmasses (Garreaud, 2007). Recent studies have postulated that changes in the strength and/or latitudinal position of the SWW over critical regions in the mid latitudes of the Southern Ocean have driven ocean-atmosphere CO_2 exchange via wind-driven upwelling of CO_2-rich deep waters in the Southern Ocean during the last glacial-interglacial transition (Anderson et al., 2009; Denton et al., 2010; Fletcher and Moreno, 2011; Toggweiler et al., 2006). Despite considerable advances in our comprehension of long-term climatic change in the mid-latitudes of the Southern Hemisphere, our understanding of the evolution of the SWW and their

* Corresponding author.
E-mail address: william.henriquezgonzalez@unimelb.edu.au (W.I. Henríquez).

https://doi.org/10.1016/j.quascirev.2023.108315
Received 21 June 2023; Received in revised form 6 September 2023; Accepted 12 September 2023
Available online 21 September 2023

underlying mechanisms since and during the LGM is still limited.

Western Tasmania (41–44°S, Fig. 1), in southeast Australia, exhibits the strongest correlation between changes in the SWW and terrestrial climate in the Southern Hemisphere over the historical period (Gillett et al., 2006). Thus, this region constitutes a key region for tracking long-term shifts in the SWW through time using the numerous lake sediment archives located in this cool temperate landscape. Stratigraphic and geomorphologic studies indicate that central-west Tasmania was partially covered by two ice caps during the LGM (Colhoun et al., 1996; Peterson and Robinson, 1969). Paleoclimate and palaeoecological studies from this region have documented a sequence of environmental changes through the LGM, the Last Glacial Termination (Termination 1 = T1, ~17.8-11.7 cal kyr BP) and the current interglacial (Holocene, ~11.7 cal kyr BP-present). Most of these studies are based on fossil pollen, and microscopic and macroscopic charcoal records deposited and preserved in lake and wetland sediments (Beck et al., 2017; Colhoun and Shimeld, 2012; Fletcher and Moreno, 2011, 2012; Fletcher et al., 2021c; Mariani and Fletcher, 2017). These records have provided insights into past changes in the structure and composition of the local and regional vegetation in response to long-term changes in human and climatic drivers (Colhoun et al., 1999; Colhoun and Shimeld, 2012; Fletcher et al., 2018, 2021c; Fletcher and Moreno, 2012; Mariani and Fletcher, 2016; Mariani et al., 2017b, 2019). To date, however, there are no continuous, well-dated and high-resolution records that

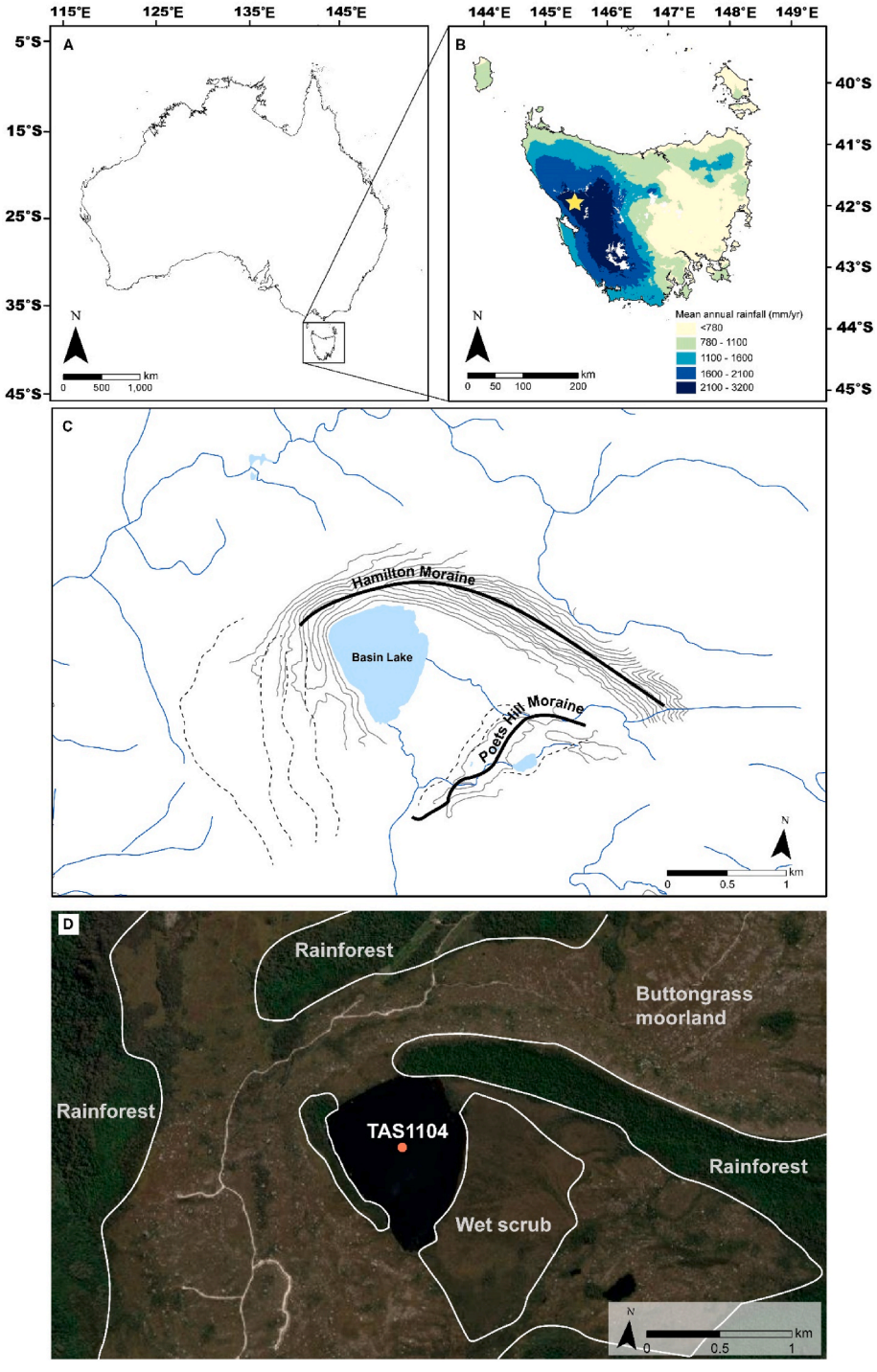

Fig. 1. (a) Map of Australia showing the location of Tasmania; (b) Map of Tasmania indicating the location of Basin Lake (yellow star) and the average annual rainfall isohyets showing the orographic rainfall gradient across the island,; (c) Location of Hamilton Moraine and Poets Hill Moraine (dark black solid lines) (Barrows et al., 2002) with 10m contours (light grey solid lines), the locations of other ice positions (dashed black lines) and location of Basin Lake; (d) Satellite image of Basin Lake indicating the location of the core site (orange dot),the core code (TAS1104) and the distribution of buttongrass moorland, wet scrub (Western wet scrub) and rainforest.

span the period from the LGM to the present from Tasmania, limiting our understanding of the nature and timing of climate- and human/disturbance-driven vegetation change during this critical phase of the Earth's past.

Here we report on high-resolution fossil pollen and macroscopic charcoal records from sediment cores obtained from Basin Lake (41°58′49.83′′S; 145°32′56.08′′E, 580 m.a.s.l., maximum depth 4 m, Fig. 1), a relatively small lake located on the West Coast Range in central-western Tasmania. We aim to examine vegetation, fire-regime and climate changes since and during the latter part of the LGM. These data allow the assessment of the following questions: i) How did the vegetation and fire-regime change during and since the late-LGM?, (ii) What was the timing and direction of paleoclimate conditions pre-, during and post-deglaciation?, and (iii) What were the main drivers of vegetation and fire regime change over the last 21,000 years?

1.1. Western tasmania

Tasmania (41–44°S; Fig. 1) is a large island located to the south of southeast Australia and is separated from mainland Australia by a shallow sea (the Bass Strait). This island is part of the Australian continental plate and is considered tectonically stable compared to other regions (Hasterok et al., 2022). Tasmania's eastern and western shores face the Tasman Ocean and the Indian Ocean, respectively, while the Southern Ocean lies to the south of this continental island. The island is bisected by a northwest-southeast mountain range, which features numerous rivers, lakes, valleys and glacial deposits formed during and following multiple Quaternary glaciations (Banks et al., 1987; Barrows et al., 2002; Colhoun et al., 1996).

Western Tasmania is a vertiginous and topographically complex landscape with a cool and hyper-humid climate dominated by the permanent influence of the SWW (Gillett et al., 2006). The presence of the northwest-southeast mountain range constitutes a formidable topographic barrier to the SWW, inducing a steep west-east orographic precipitation gradient. Mean annual precipitation in western Tasmania reaches values of ~1200 mm in the far northwest at the upper limits of the perennial SWW area of influence, while more than ~3500 mm falls on the West Coast Range, the first orographic barrier to the moisture laden SWW on their journey across Tasmania. Precipitation exceeds evaporation for most of the year. Farther to the east of the central mountain ranges and broad plateau, precipitation declines to values ~400 mm (Sturman and Tapper, 1996). Interannual climatic variability in the island is modulated by the Southern Annular Mode (SAM) and the El Niño-Southern Oscillation (ENSO), with SAM being the only statistically significant driver of precipitation in western Tasmania during the historical period (Mariani and Fletcher, 2016). Fires are ubiquitous across Tasmania and have modified the landscape since at least the arrival of people after ~40.0 cal kyr BP (Bowman, 2000; Fletcher and Thomas, 2010a). While human are almost invariably ignition sources by practicing frequent small-scale fires to maintain open vegetation to increase resource availability and promote biodiversity (Adeleye et al., 2021; Bowman and Brown, 1986; Fletcher and Thomas, 2010b; Ingles, 1985; Jackson and Bowman, 1982), fire occurrence through time in this region is strongly modulated by climate, with high (low) fire activity associated with drier (wetter) conditions that are statistically correlated with southward (northward) displacement of the SWW that occur during positive (negative) phases of SAM (Mariani and Fletcher, 2016).

The composition and distribution of plant communities across Tasmania is controlled by steep west-east and altitudinal climatic gradients, fire and geology (Bowman and Jackson, 1981; Harris and Kitchener, 2005; Kirkpatrick and Dickinson, 1984; Reid et al., 1999). The dominant vegetation units present in western Tasmania in the absence of regular disturbance by fire are (Harris and Kitchener, 2005): i) Lowland rainforest (up to 620 m.a.s.l.) that is characterized by the presence of *Nothofagus cunninghamii*, accompanied by *Phyllocladus aspleniifolius*, *Lagarostrobos franklinii*, *Athrotaxis selaginoides*, *Eucryphia lucida*, *Atherosperma moschatum* and *Anodopetalum biglandulosum*; ii) Montane rainforest (620–850 m.a.s.l.) which includes *Athrotaxis cupressoides*, *Athrotaxis selaginoides* (Cupressaceae) and *Nothofagus gunnii*; iii) Subalpine forest (850–950 m.a.s.l.) that features several species of endemic conifer, including *Pherosphaera hookeriana*, *Microcachrys tetragona*, *Diselma archeri*, *Athrotaxis cupressoides*, *Athrotaxis laxifolia*, and *Athrotaxis selaginoides*. *Eucalyptus nitida* woodland, scrub and heath occurs at the highest elevation; and iv) Alpine vegetation (above 950–1030 m.a.s.l.) includes herbs, shrubs and conifer heath, with *Donatia novae-zelandiae*, *Plantago* spp., *Nothofagus gunnii* and *Astelia alpina* commonly occurring in alpine wetlands (Kirkpatrick, 1982). In fire effected areas, sclerophyll fire-adapted species expand at the expense of fire-sensitive rainforest species, including the dominant vegetation type across western Tasmania today: Buttongrass Moorland. Buttongrass Moorland occurs and dominates in areas of high fire frequency (<20 years interval) that are both well- and poorly-drained (Bowman and Jackson, 1981; Jackson, 1968). This vegetation type is characterized by the sedge *Gymnoschoenus sphaerocephalus* (Cyperaceae), accompanied by *Epacris*, *Sprengelia*, *Richea*, *Dracophyllum*, *Monotoca* (Ericaceae), *Melaleuca*, *Leptospermum*, *Baeckea* (Myrtaceae), *Baumea*, *Schoenus* (Cyperaceae), *Restio* and *Empodisma* (Restionaceae) (Jarman et al., 1988). While Buttongrass Moorland has many identified sub-classes, the dominant and most palynologically distinct types are western buttongrass moorland and eastern moor. Western buttongrass moorland (commonly referred to as Blanket Moor) is found in perennially waterlogged parts of the landscape where it forms extensive treeless peatlands and includes species such as *Leptospermum nitidum, Melaleuca squamea* and *Sprengelia incarnata*. Eastern Moor occurs in soils that are better drained with lower species diversity than Blanket Moor, including *Baeckea gunniana*, *Epacris gunni*, *Helichrysum dealbatum* and Poaceae species (Harris and Kitchener, 2005).

1.2. Basin lake

This study focuses on Basin Lake, a small closed-basin lake located ~26 km inland from the west coast of Tasmania in what is today known as the West Coast Range (Fig. 1). Basin Lake lies at the southern section of a long (~12 km), narrow (~3 km) and broadly flat plain that flanks the mid elevations of the western slopes of West Coast Range. The Tyndall Plateau (~1000 m.a.s.l), which hosted a small LGM ice cap (Barrows et al., 2002; Colhoun, 1985), looms above the plain to the east, while the Henty River Valley plunges to ~100 m.a.s.l. immediately to the west. Basin Lake is situated at ~578 m.a.s.l. over Pleistocene glacial deposits that overlie Cenozoic bedrock. The lake is located between two glacial moraines emplaced by ice that formed to the east on the Tyndall Plateau: the Hamilton End Moraine to the west of the lake and most distal to the Tyndall Range, and the Poets Hill Moraine to the east of the lake and most proximal of the two moraines to the Tyndall Range ice source (Barrows et al., 2002). Cosmogenic dating of these moraines by Barrows et al. (2002) has revealed a complex of ice abandonment ages from the Hamilton End Moraine, indicating phases of emplacement and subsequent abandonment between ~190.0-350.0 cal kyr BP. In contrast, a cosmogenic age of ~17.4 cal kyr BP at the Poets Hill moraine which indicates the maximum extent of the restricted LGM ice advance at this location (Fig. 1). Average annual rainfall exceeds 3600 mm on the West Coast Range, with the closest weather station to Basin Lake recording 2400 mm annually (Queenstown ~11 km south). Temperature ranges between 5-7 °C in winter (June to August) and 14–16 °C in summer (December to February) (Australian Bureau of Meteorology, http://www.bom.gov.au/).

The local vegetation along the flat plain, the slopes of the West Coast Range and the Tyndall Plateau is dominated by Western Buttongrass moorland communities that are interspersed with small pockets of rainforest where topography has afforded protection from fire (such as along the south facing portions of the Hamilton End Moraine wall) (Fig. 1). Alpine vegetation communities dominate at higher elevations.

Immediately to the west along the main axis of wind flow to the site, dense cool temperate rainforest cloaks the Henty River Valley and further to the west.

2. Material and methods

We obtained multiples sediment cores from the deepest sector of Basin Lake (4 m water depth) during December 2011 using an anchored platform equipped with a 6.8-cm diameter water interface piston core and a 5-cm diameter Livingston piston corer. All sediment cores were transported from the field and stored at 4 °C at the University of Melbourne. We sub-sampled the composite stratigraphy of Basin Lake record for chronologic control, fossil pollen and macroscopic charcoal analyses. The chronology of the record is constrained by AMS radiocarbon dates and lead-210 dates obtained from bulk organic samples retrieved from 1-cc thick sections (Tables 1 and 2). We calibrated the radiocarbon dates using the SHCal20 (Hogg et al., 2020) included in CALIB 8.1 (Reimer et al., 2013) and developed a Bayesian age model using the Bacon package *v.3.0.0* for R *v.4.1.3* (Blaauw and Christen, 2011) (Fig. 2).

We took 0.5-cc sediment samples obtained from 0.5 and 1-cm thick section spaced at intervals that range from 0.5 to 2 cm for pollen analysis. The pollen samples were processed following a modified version of a standard procedure, which includes 10% KOH, 40% HF and acetolysis (Faegri et al., 1989). The pollen concentrates were mounted on glass slides using glycerol and analysed at 400X magnification using a compound light microscope. For each sample, a minimum of 300 pollen grains from trees, shrubs and herbs (terrestrial pollen) were identified. We calculated the percent abundance of each terrestrial taxon relative to the terrestrial pollen sum. The percent abundance of pteridophytes and aquatic plants was calculated in reference to the sum total pollen (terrestrial pollen + pteridophytes + aquatic). Sum and percentage of all taxa were calculated and presented as pollen percentage diagrams using the software Tilia 2.6.1 (https://www.tiliait.com/) (Fig. 3). We defined pollen zones with the aid of a stratigraphically constrained CONISS ordination applied to all terrestrial taxa with abundance values $\geq$ 2% (Grimm, 1987). We conducted a broken stick model (Bennett, 1996) to determine the number of statistically significant pollen assemblage zones using the package rioja *v. 0.9.15.1* in R *v.4.1.3* (Juggins, 2016), considering all terrestrial taxa with abundance values $\geq$ 2%. We standardized the original percent abundance of selected taxa to the mean of the entire record and the Holocene (last 12,000 years) to characterize values around the mean through these distinct climatic intervals and summarize the major trends in the pollen record. We performed change point analyses on these standardized values to detect statistically significant changes in the temporal dataset using the changepoint package *v. 2.2.4* in R *v.4.1.3* (Killick and Eckley, 2014).

We identified the palynomorphs based on modern reference samples stored at the University of Melbourne, along with published descriptions and keys (Macphail and Hope, 2018; Punt et al., 2007; Thornhill et al., 2012a, 2012b, 2012c, 2012d). The majority of the identification was done at family or genus level, but in some cases to the specie level (*Pherosphaera hookeriana*, *Nothofagus gunnii*, *Phyllocladus aspleniifolius*, *Nothofagus cunninghamii*, *Agastachys odorata*, *Bauera rubioides*, *Banksia marginata*, *Gymnoschoenus sphaerocephalus*). The palynomorph *Pomaderris apetala*-type includes the subspecies *Pomaderris apetala* Labill. subsp. *maritima* and *Pomaderris apetala* Labill. subsp. *apetala*.

We analysed macroscopic charcoal content of 1.25-cc sediment samples taken at continuous contiguous 1-cm thick sections throughout the sediment cores. The samples were rinsed in a 10% KOH solution, sieved through 125 and 250-μm meshes and counted under a stereoscope at 10X magnification. The counts of charcoal are presented as charcoal accumulation rates (CHAR = particles*cm^{-2}*year^{-1}) (Fig. 4). We performed time-series analysis on the charcoal record to detect statistically significant local fire events, and their frequency and magnitude using the software CharAnalysis (Higuera et al., 2009). We interpolated the charcoal record to consistent time intervals based on the median time resolution and defined background charcoal using a Lowess robust-to-outliers and smoothing windows of 1000 years. We used a locally defined threshold to identify charcoal peaks exceeding the 99th percentiles distribution of positive residuals, utilising a Gaussian mixture model.

Based on surface-modern pollen data from several sites from Tasmania (D'Costa and Kershaw, 1997; Fletcher et al., 2021b; Fletcher and Thomas, 2007; Kershaw et al., 1994; Thomas and Hope, 1994), we calculated threshold pollen values (TPV) to illustrate changes of the palynologically inferred plant communities (Fig. 5). We grouped and summed modern pollen abundance of taxa characteristic of rainforest, grassland (Poaceae) and moorland communities in each site. Then, we summed each group of all sites and calculated their means, standard deviations and absolute minimum values which represent the TPVs or the pollen abundance required for the extant of local rainforest, moorland or grassland communities. We interpret reconstructed pollen abundance values from palynological records above the TPVs as indicative of local presence of these plant communities, values below the TPVs are interpreted as extra local signal of these plant communities.

3. Results

3.1. Stratigraphy and chronology

The sedimentary record from Basin Lake has a total composite length of 306 cm and combines the water-sediment interface core TAS1104SC1 and cores from the series TAS1104LCA (segments 2 to 5). The sediment cores were correlated by overlapping different cores with the aid of the charcoal record. The lowermost portion of the record consists of a basal unit of organic silt between 306-296 cm, followed by organic-rich lake mud (gyttja) from 296 cm to the top of the record (Fig. 3). The chronology of Basin Lake record is constrained by 9 AMS radiocarbon dates, along with 4 lead-210 dates (Tables 1 and 2). The lowermost radiocarbon date yielded an age of ~20.4 cal kyr BP (2σ: ~20.6–20.2 cal kyr BP), followed by progressively younger ages toward the top of the record (Table 2). The combined radiocarbon and lead-210 age-depth model, along with the sediment stratigraphy suggest continuous sedimentation in a constant lacustrine environment during the last ~21,000 years (Fig. 2).

3.2. Pollen record

The pollen record from Basin Lake comprises 197 samples that span the last ~21,000 years with a median time resolution between pollen samples of ~46 years. We divided the pollen record into 6 palynological

Table 1
Lead-210 dates from Basin Lake.

Laboratory code	Core code	Material	Depth (cm)	Total 210 Pb (Bq/kg)	Unsupported 210 Pb Decay (Bq/kg)	Calculated CRS Age (as Calendar year CE)	Age (cal year BP)	1σ error
P063	TAS1104SC1	Bulk	0.25	471.7	467	2001	−57	4.1
P064	TAS1104SC1	Bulk	2.25	386.1	378	1975	−25.3	8.9
P065	TAS1104SC1	Bulk	4.25	133.1	125	1944	6.5	15.6
P066	TAS1104SC1	Bulk	6.25	53.3	45	1912	38.2	22.5

Table 2
Summary of radiocarbon dates obtained from Basin Lake. The dates were calibrated to calendar years before present (cal yr BP) using the CALIB 8.1 program.

Laboratory code	Core code	Material	Depth (cm)	^{14}C yr BP	±1 σ error	2σ range cal yr BP	Median probability cal yr BP
TAS1104SC1-1	TAS1104SC1_22–22.5	Bulk	22.25	1750	25	1539–1699	1616
TAS1104SC1-2	TAS1104SC1_34–34.5	Bulk	34.25	2470	25	2353–2701	2476
TAS1104SC1-3	TAS1104SC1_72–72.5	Bulk	72.25	4900	30	5478–5710	5595
TAS1104SC1-5	TAS1104LCA2_83-84	Bulk	117	6447	38	7257–7425	7338
TAS1104SC1-6	TAS1104LCA3_68-69	Bulk	189	8800	60	9548-10,120	9772
TAS1104SC1-7	TAS1104LCA4_37-38	Bulk	240	10,120	57	11,318–11,867	11,636
TAS1104SC1-8	TAS1104LCA4_59-60	Bulk	262	10,952	69	12,739–13,061	12,842
TAS1104SC1-9	TAS1104LCA5_14-15	Bulk	291	14,268	38	17,103–17,413	17,286
TAS1104SC1-10	TAS1104LCA5_23-25	Bulk	301	16,930	80	20,181–20,597	20,415

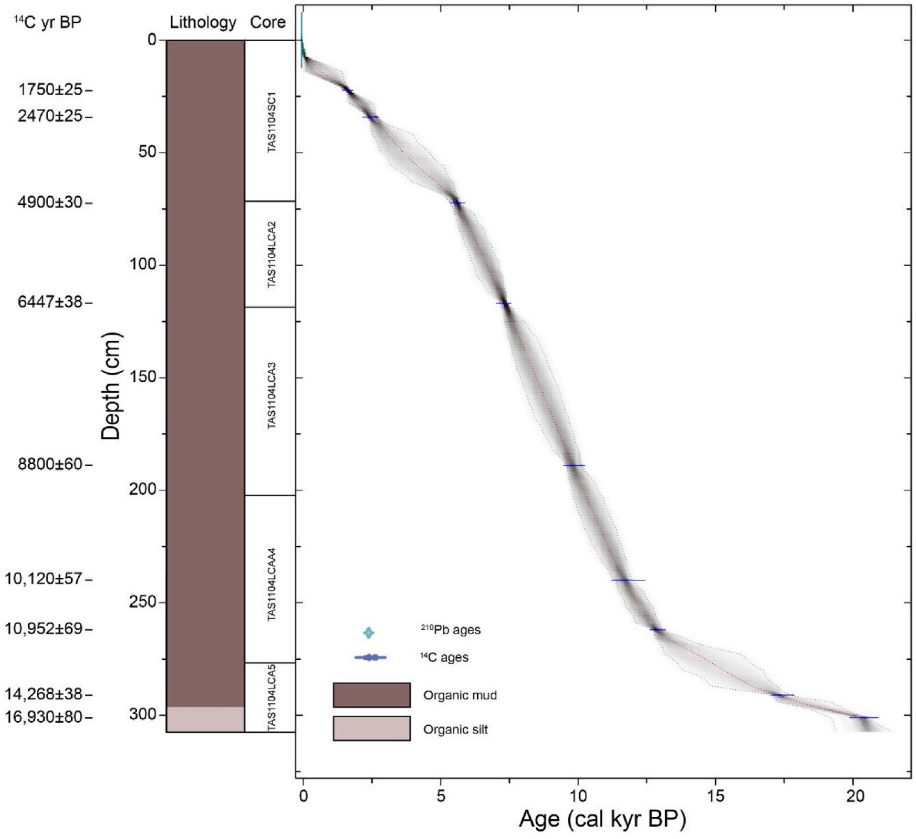

Fig. 2. Age model of Basin Lake record, along with the identity and stratigraphic span (black lines between cores) of each core segment, stratigraphic column and radiocarbon dates. The probability distribution of each calibrated radiocarbon date is shown in blue, the red line represents the median probability of the age model and the 95% confidence interval of the Bayesian age model is represented in grey.

zones based on the most conspicuous changes in the pollen stratigraphy as determined with the aid of a stratigraphically constrained CONISS ordination and a broken stick model (Fig. 3). Below, we describe each zone indicating their depth and age ranges, the three most abundant terrestrial taxa and less-abundant taxa with their mean percent abundance in parenthesis, supplemented with statistically significant changes (changepoint) and our vegetation threshold analysis (TPV) (Figs. 3 and 5).

Zone BL-1 (306-292 cm, ~21.0-17.5 cal kyr BP) is characterized by Poaceae (32.4%), Asteraceae subfamily Asteroideae (15.5%) and *Eucalyptus* spp. (11%), accompanied by relatively low abundance of arboreal pollen (>30%). We note decreasing trends in *Plantago* spp. (4%), Amaranthaceae (9.1%) and Asteraceae subfamily Asteroideae. Asteraceae low spine (2%) shows its highest abundance of the entire record at the beginning of this zone, followed by its decrease and disappearance. Moorland indicators show relatively low percent abundances with values above the TPV (Moorland taxa; μ: 30.3%, 1σ: 12.8%, min.: 2.1%) that persist until the present. We highlight a ~2%-plateau in *G. sphaerocephalus* and traces abundance in *Banksia marginata* (<0.5%) and *Melaleuca* (<1%), the latest showing a low-magnitude statistically significant increase at ~18.8 cal kyr BP (2σ; ~19.7-17.3 cal kyr BP). Casuarinaceae (5.1%) and Cupressaceae (7.2%) show increasing trends, the latest declining abruptly near the end of this zone. The macrophyte Cyperaceae (4.3%) exhibits its highest abundance of the entire record at the start of this zone, followed by a statistically significant decline at ~19.2 cal kyr BP (2σ; ~20.1-17.3 cal kyr BP), and continuing with relatively low values until the end of this zone. The aquatic species *Isoëtes* spp. (11%) shows low abundance at the beginning of this zone, followed by a statistically significant increase at ~19.7 cal kyr BP (2σ; ~20.7-17.3 cal kyr BP) that led to its highest abundance of entire record. While Poaceae exhibits abundance above the TPVs (Grassland taxa; μ: 34.2%, 1σ: 14.1%, min.: 7.8%), Rainforest taxa (4%) present values below the TPVs (Rainforest taxa: μ: 79.0%, 1σ: 71.6%, min.: 64.1%).

Zone BL-2 (292-271 cm, ~17.5-14.0 cal kyr BP) shows dominance of *N. cunninghamii* (17%), *P. aspleniifolius* (16.7%) and Poaceae (8.7%), featuring increases in the percent abundance in *P. aspleniifolius*,

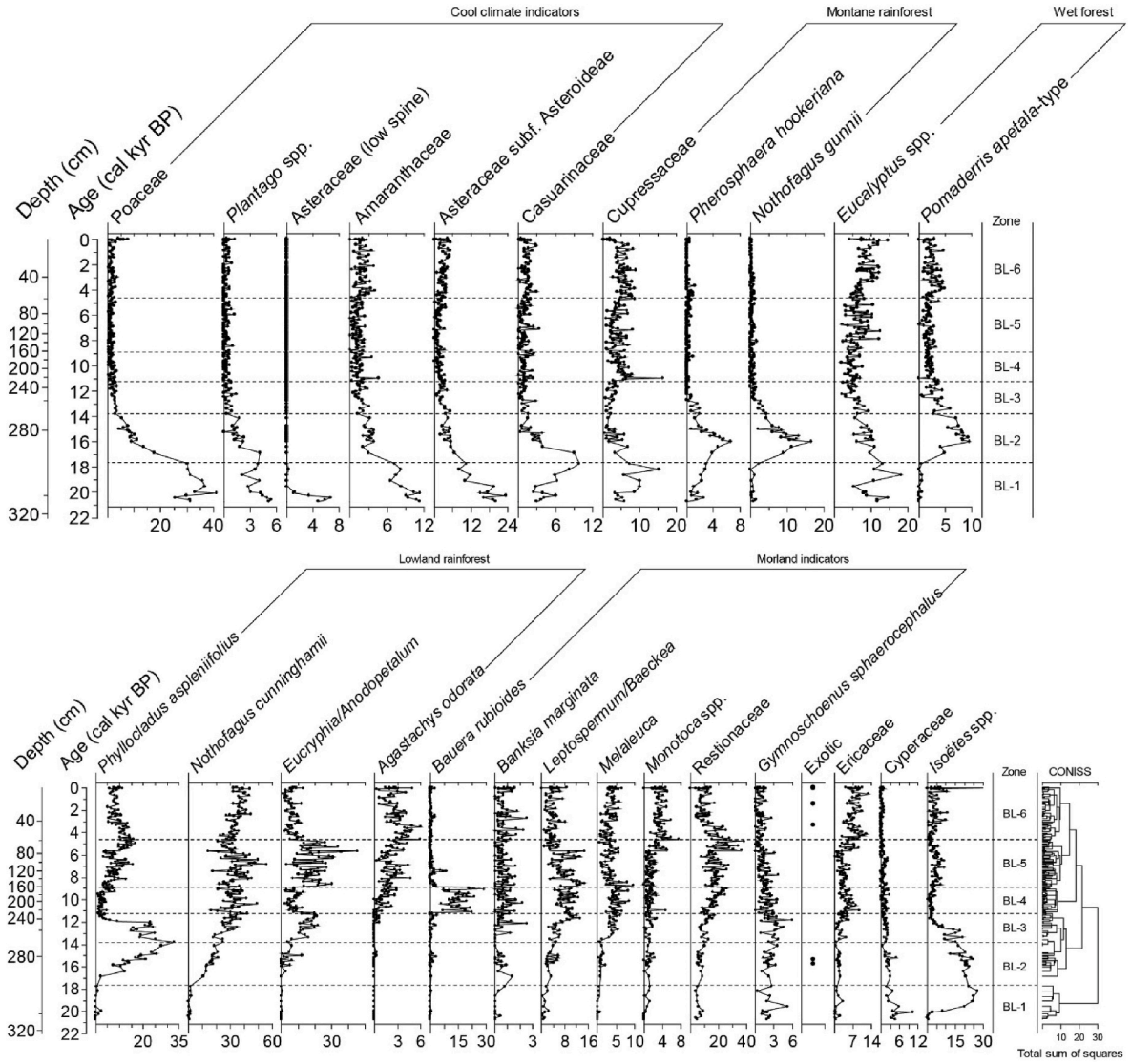

Fig. 3. Percentage pollen diagram from Basin Lake. The primary y axis shows the composite depth of the record, the secondary y axis indicates the age scale. The labels on the right indicate the identity and stratigraphic span (black dashed horizontal lines) of each pollen assemblage zone. Note the difference in scale between taxa.

N. cunninghamii, *Pomaderris apetala*-type (7.1%) and *Eucryphia/Anodopetalum* (3%) at the expense of *Eucalyptus* spp. (8.5%) and the cold-resistant taxa Poaceae, *Plantago* spp. (1.5%), Amaranthaceae (3%), Asteraceae subfamily Asteroideae (4.4%) and Casuarinaceae (2.7%) and Cupressaceae (2.7%). *P. hookeriana* (3.5%) and *N. gunnii* (8.7%) show a rapid increase at the beginning of this zone, followed by their sustained decline. *G. sphaerocephalus* continues in a ~2%-plateau showed in the previous zone, whilst *B. marginata* (<1%) reappears in the record exhibiting a decreasing trend that led to its disappearance at the end of this zone. Cyperaceae (2.2%) and *Isoëtes* spp. (19.6%) exhibit statistically significant declines at ~14.8 cal kyr BP (2σ; ~16.6-12.3 cal kyr BP) and ~15.0 cal kyr BP (2σ; ~17.0-12.6 cal kyr BP), respectively, whilst *Leptospermum/Baeckea* shows a statistically significant increase at ~15.7 cal kyr BP (2σ; ~17.5-14.5 cal kyr BP). Rainforest pollen shows abundance below the TPVs and Poaceae exhibits abundance above the TPVs until ~15.0 cal kyr BP continuing with abundance below the TPVs until the present.

Zone BL-3 (271-227 cm, ~14.0-11.2 cal kyr BP) exhibits the dominance of *N. cunninghamii* (29.5%), *Eucryphia/Anodopetalum* (15.9%) and *P. aspleniifolius* (13%). *N. cunninghamii* continued its increasing trend from the previous zone, whilst *Eucryphia/Anodopetalum* shows a rapid rise and *P. aspleniifolius* features prominent declines between ~14.0-12.5 and ~12.0-11.2 cal kyr BP. *Leptospermum/Baeckea* and *Melaleuca* increase, exhibiting statistically significant rises at ~12.1 cal kyr BP (2σ; ~12.9-11.3 cal kyr BP) and ~13.6 cal kyr BP (2σ; ~15.4-11.9 cal kyr BP), respectively. Cold-resistant taxa show their lowest abundances of the entire record (<15%). *G. sphaerocephalus* (3%) shows a slight increasing trend, whits *B. marginata* (<1%) reappears in the record. *Isoëtes* spp. (6.5%) shows a rapid statistically significant decline at ~12.2 cal kyr BP (2σ; ~13.1-11.3 cal kyr BP). Rainforest pollen shows abundance above the TPVs at ~12.5 cal kyr BP.

Zone BL-4 (227-159 cm, ~11.2-8.9 cal kyr BP) is dominated by *N. cunninghamii* (31.4%), Restionaceae (17.3%) and *Bauera rubioides* (15.3%). *Eucryphia/Anodopetalum* (7%) shows an abrupt decline at the commence of this zone. At the same time, Cupressaceae (5.1%) exhibits a pick abundance, followed by its sustained decrease. *B. rubioides* (15.2%) rises and declines abruptly at the beginning and end of this zone, respectively, exhibiting its highest abundance of the entire record. *Agastachys odorata* (1.2%) starts an increasing trend, *G. sphaerocephalus* (3%) shows a rapid decline, and *Eucalyptus* spp. (4.7%) and *P. aspleniifolius* (3%) present their lowest percent abundance of the entire record. *Isoëtes* spp. (4%) remains relatively low during this zone.

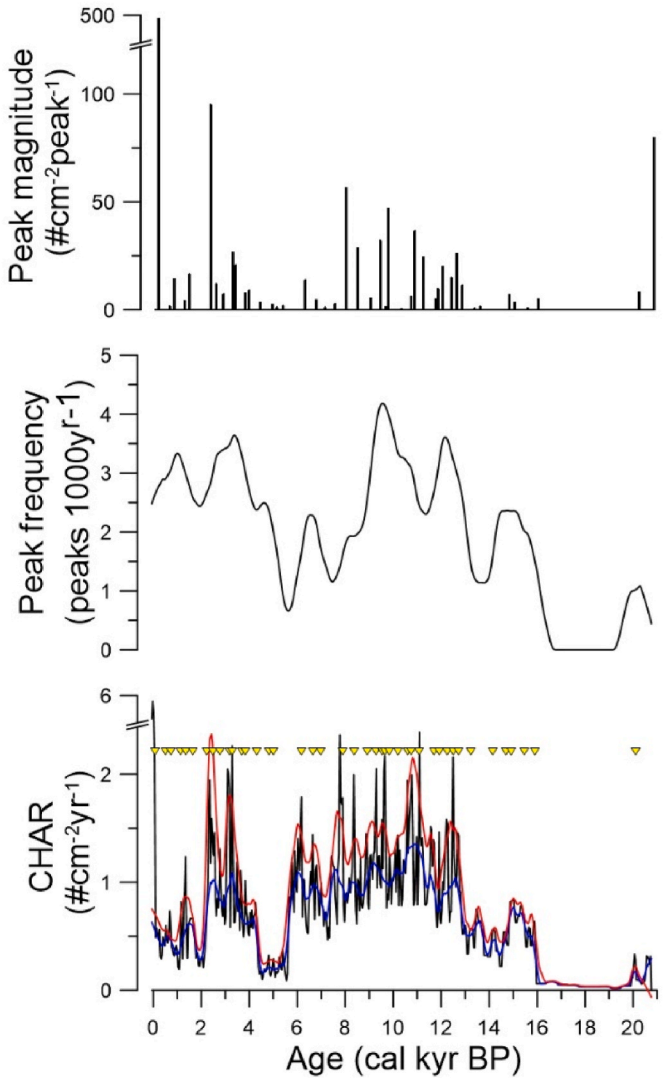

Fig. 4. Macroscopic charcoal accumulation rate (CHAR) from Basin Lake and time series analysis using CharAnalysis, showing the calculated background (blue line) using a lowess robust to outliers, the local defined threshold (red line), and the statistically significant charcoal peaks (yellow triangles), peak frequency and magnitude.

Rainforest pollen shows abundance below the TPVs along this zone.

Zone BL-5 (159-59 cm, ~8.9-4.5 cal kyr BP) features the dominance of *N. cunninghamii* (32.7%), Restionaceae (19.1%) and *Eucryphia/Anodopetalum* (19.1%). *P. aspleniifolius* (8.7%) exhibits a sustained increase, whilst *Eucalyptus* spp. (6.3%) and *Eucryphia/Anodopetalum* show increasing trends with fluctuations. Cool climate indicators show low abundance (<15%). *Monotoca* spp. (1.8%) and Ericaceae (3.7%) show sustained increases at the end of this zone. *Melaleuca* (3.3%) and *Leptospermum/Baeckea* (7.2%) exhibit statistically significant declines at ~8.3 cal kyr BP (2σ; ~9.7-7.2 cal kyr BP) and ~5.6 cal kyr BP (2σ; ~6.1-5.1 cal kyr BP), respectively. The aquatics *Isoëtes* spp. (4.4%) shows a statistically significant increase at ~8.7 cal kyr BP (2σ; ~10.0-7.4 cal kyr BP), followed by a statistically significant decline at ~5.1 cal kyr BP (2σ; ~6.0-3.8 cal kyr BP), whilst Cyperaceae (<1%) exhibits a statistically significant decline at ~6.3 cal kyr BP (2σ; ~7.5-5.4 cal kyr BP). Rainforest pollen shows abundance above the TPVs along this zone.

Zone BL-6 (59-0 cm, ~4.5 cal kyr BP-present) indicates dominance of *N. cunninghamii* (35.2%), Restionaceae (11.6%) and *P. aspleniifolius* (9.2%), with increasing trends in *N. cunninghamii* and *Eucalyptus* spp. (8.5%) and decreasing trends in *P. aspleniifolius*, *Eucryphia/Anodopetalum* (6.5%) and Restionaceae. Amaranthaceae (2%), Asteraceae subfamily Asteroideae (3%), Casuarinaceae (1.3%) and Cupressaceae (5%) increase in this zone. *P. apetala*-type (2.5%) and *Agastachys odorata* (2.9%) exhibit rapid rises at the beginning of this zone, followed by their sustained decline. *Monotoca* spp. and Ericaceae achieved a 3.4% and 7.4% plateau, respectively. *Isoëtes* spp. shows a statistically significant increase at ~3.9 cal kyr BP (2σ; ~5.7-2.2 cal kyr BP), remaining in a 5% plateau with variations that range between ~10% and ~2%. Exotic taxa appear in the record (*Pinus*, Asteraceae subfamily Cichorioideae and *Rumex*) during the last ~100 years. Rainforest pollen shows abundance below the TPVs along this zone.

3.3. Macroscopic charcoal

The macroscopic Charcoal Accumulation Rates (CHAR) record from Basin Lake (Fig. 4) comprises 377 samples, with a median temporal resolution between charcoal samples of ~43 years. The record starts with a discrete peak in CHAR between ~21.0-20.0 cal kyr BP, followed by very low CHAR between ~20.0-16.0 cal kyr BP, a sudden rise between ~16.0-14.9 cal kyr BP, a decline between ~14.9-12.8 cal kyr BP, and a multi-millennial interval of high CHAR between ~12.8-5.7 with the highest values between ~12.8-8.9 cal kyr BP. The latest multi-millennial interval was followed by low CHAR between ~5.7-4.3 cal kyr BP, increased values between ~4.3-2.2 cal kyr BP, relatively low values with variations between ~2.2-0.1 cal kyr BP and a peak during the last ~100 years. Time series analysis of these data reveals 42 statistically significant charcoal peaks, interpreted as local fires events (Fig. 4). The record shows an initial isolated event at ~20.1 cal kyr BP, followed by clustering of events between ~16.0-12.8 (6 events), ~12.8-8.9 (14 events), ~8.9-6.2 (5 events) and ~5.0-4.3 cal kyr BP (3 events), and during the last ~4300 years (14 events). The charcoal peak frequency and magnitude parameters show relatively low values between ~21.0-20.0, ~14.9-12.8 and ~5.7-4.3 cal kyr BP, intermediate values between ~16.0-14.9 and ~8.9-5.7 cal kyr BP, and highest values between ~12.8-8.9 cal kyr BP and during the last ~4300 years (Fig. 4).

4. Discussion

4.1. Vegetation, fire and climate history

The Basin Lake pollen and charcoal data reveal changes in the structure and composition in plant communities and biomass burning in central-west Tasmania over the last ~21,000 years. Our data indicate an open landscape dominated by cold-resistant alpine vegetation (Poaceae, Asteraceae, Amaranthaceae, Casuarinaceae and *Plantago* spp.) between ~21.0-17.7 cal kyr BP. The co-occurrence of *G. sphaerocephalus* and Poaceae indicate the presence of Eastern Moor at the site (Fletcher and Thomas, 2007). The occurrence of fire-dependent buttongrass moorland, despite the low charcoal input at this time (a metric of amount of biomass burned) (Power et al., 2008; Whitlock and Larsen, 2001), likely reflects a low vegetation biomass and consequent low charcoal production. Indeed, this mix of vegetation types, along with the overall absence of lowland rainforest species and the high values of *Isoëtes* spp. spores, a littoral aquatic macrophyte that prefers minerogenic lakeshores and clear water (Chappuis et al., 2015; Mariani et al., 2018; Riera et al., 2017), suggests a low biomass landscape under a cool glacial climate regime at the end of the LGM (Figs. 3 and 5). The absence of trees at the site, which were either confined to microclimatic refugia in topographically favourable locations or at lower elevations, implies a lowering of the treeline of at least ~500 m relative to today between ~21.0-17.7 cal kyr BP. Applying an adiabatic lapse rate of 0.7 °C per 100 m (Nunez, 1988), we infer a temperature depression of at least ~3.5 °C relative to modern during this period.

Within this glacial-cold late-LGM interval we detect intensification of cold conditions between ~20.0-17.7 cal kyr BP, implied by peak abundance in Poaceae and Casuarinaceae and a decline in less cold-

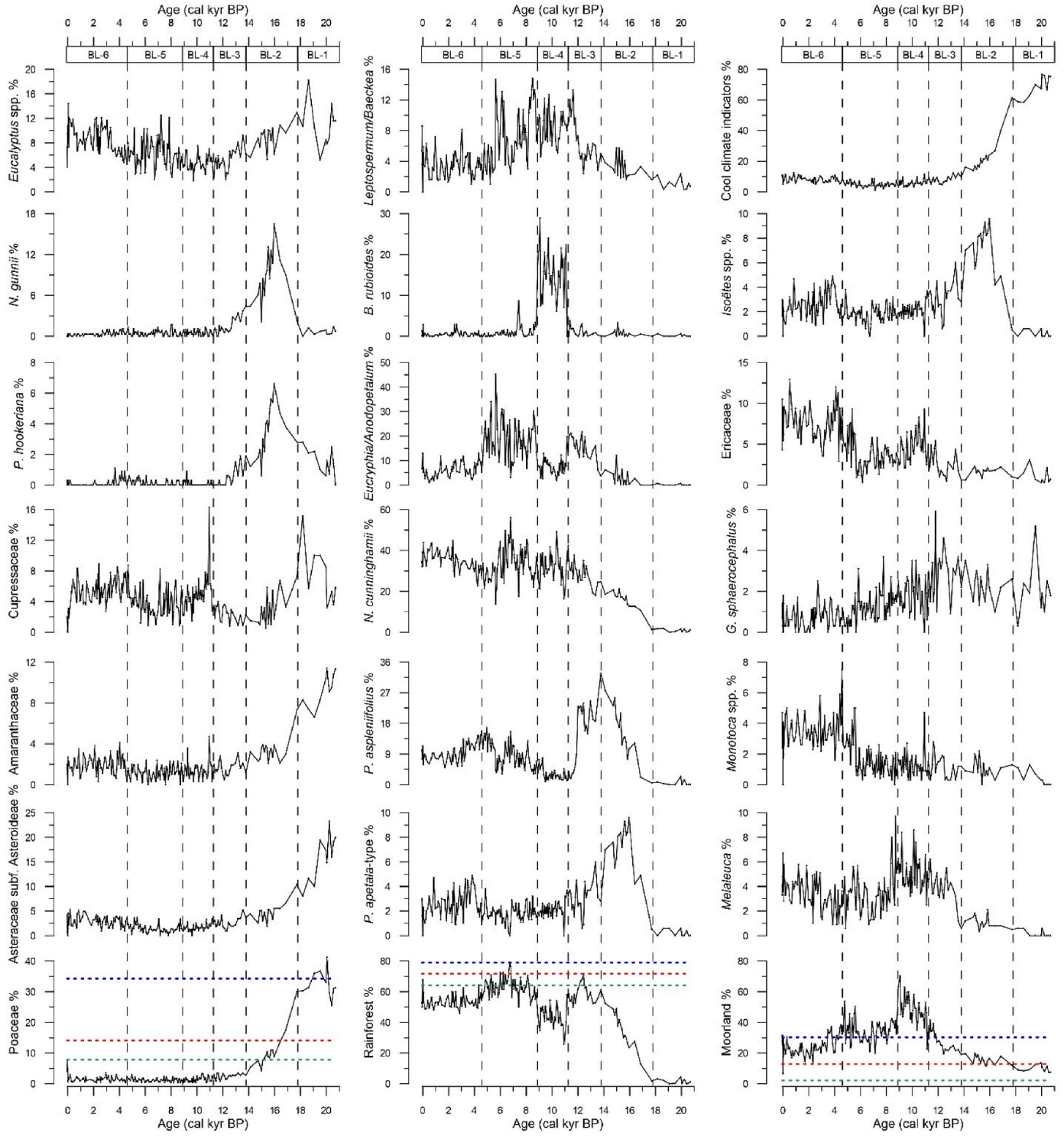

Fig. 5. Summary of pollen percentage from Basin Lake record. The dashed vertical lines constrain the timing of the pollen zones, indicating their identities in boxes below the upper X axis. The blue, red and green dashed horizontal lines indicate the mean pollen values of modern pollen abundance for each plant communities, standard deviation, and absolute minimum values (TPV), respectively.

tolerant taxa (Asteraceae low spine, *Plantago* spp., Amaranthaceae, Asteraceae subf. Asteroideae) (Fig. 3). At the same time, we infer oscillations in water level from shifts in the macrophyte Cyperaceae. We interpret initially high Cyperaceae between ~21.0-20.0 cal kyr BP (Fig. 3) as reflecting centripetal contraction of the lake margin toward the depositional center of the lake (our core site). A reversal of this trend between ~20.0-17.7 cal kyr BP suggests a shift to higher lake levels during this phase. This inference of higher lake levels is consistent with the sharp increase in the aquatic macrophyte *Isoëtes* spp. at this time (Fig. 3). In sum, we identify an initial phase of relatively cold and dry conditions between ~21.0-20.0 cal kyr BP that resulted in low lake levels, followed by a decline in temperature and an increase in available moisture between ~20.0-17.7 cal kyr BP that led to major expansion of cold-resistant herbs and a rise in lake levels during the terminal phase of the LGM.

A shift from an open cold-climate landscape dominated by alpine

vegetation towards an open warm-climate landscape and an increase in arboreal taxa is evidenced by a rapid increase in pollen from forest taxa at ~17.7 cal kyr BP at the expense of cold-resistant alpine herbs and shrubs (Figs. 3 and 5), marking the onset of T1 at this site. This vegetation change was characterised by a local upslope displacement of local cold-adapted plant taxa with poor pollen dispersal capabilities (*N. gunnii and P. hookeriana*; Fletcher and Thomas, 2007) between ~17.7-16.0 cal kyr BP, in conjunction with the expansion of well-dispersed and more thermophilous plant taxa with regionally dispersed pollen types at lower altitudes (such as forest taxa *N. cunninghamii, P. aspleniifolius* and *P. apetala*). Locally, we observe the persistence of Eastern Moor vegetation and muted biomass burning between ~17.7-16.0 cal kyr BP (Figs. 3 and 4). These data suggest low peat cover within the area and the persistence of relatively open conditions with limited fuel available for ignition under warming and a relatively humid climate during the early stages of T1.

Our data indicate a continued expansion of arboreal cover between ~16.0-14.9 cal kyr BP, marked by an increase in the hygrophilous and cold-resistant rainforest pioneer tree *P. aspleniifolius*, along with *P. apetala*, another early forest coloniser in Tasmanian wet forests (Fletcher and Thomas, 2007; Read and Busby, 1990). These increases come at the expense of cold climate shrub, herb and tree taxa (Fig. 3) and reflect the response of lower altitude forests systems to the continued increase in temperature and moisture through T1. The sudden rise in local fire activity between ~16.0-14.9 cal kyr BP (Fig. 4) in the context of an expansion of local arboreal vegetation and high moisture suggests a shift to a higher biomass system with more fuel available for burning. The continued presence of people in the local area (Cosgrove, 1999) provided ample ignition sources that was independent of climate (i.e., lightning) in this very wet landscape. Thus, the fire activity at this site reflects both the leveraging by people of climate to affect their cultural and economic strategies and the long-term modulation of human burning by climatic and biomass controls (Fletcher and Thomas, 2010b; Mariani and Fletcher, 2017).

We observe the expansion and establishment of *P. aspleniifolius*-dominant rainforest in areas protected from fire along with a reduction in biomass burning between ~14.9-12.8 cal kyr BP (Figs. 3 and 4). We interpret these changes as a shift to colder and wetter conditions between ~14.9-12.8 cal kyr BP that interrupted the post glacial warming trend. This was followed by a shift towards *N. cunninghamii*-dominated rainforest in the region in concert with an increase in biomass burning at ~12.8 cal kyr BP. Because *N. cunninghamii* is found in less cold and wet areas relative to *P. aspleniifolius*, we interpret these data as a warmer and relatively drier climate. Despite a dominance by over-represented arboreal pollen types, the TPV analysis indicates local occurrence of moorland vegetation through this phase (Fig. 5), accounting for the paradoxical cooccurrence of pyrophobic rainforest and fire in the landscape. Continued warming and a shift to relatively drier conditions drove a further increase in biomass burning between ~11.1-8.9 cal kyr BP, with a reduction in rainforest suggesting an increased efficacy of fire under a drier climate. These shifts in temperature and fire drove a compositional shift in rainforest, with a sharp reduction in rainforest and the replacement of *P. aspleniifolius* with a simpler *N. cunninghamii* forest type (Figs. 3 and 5). Burning of rainforest is indicated by the sharp increase in *B. rubioides* at ~11.1 cal kyr BP, a forest edge species that thrives in the ecotone between forest and moorland. Within the moorland vegetation, the increase in *Leptospermum/Baeckea*, *Melaleuca* and Ericaceae reflect a compositional shift from Eastern Moor moorland to Blanket Moor moorland between ~12.8-8.9 cal kyr BP (Fletcher and Thomas, 2007) (Figs. 3 and 5), suggesting the development of more extensive peat systems under the moorland vegetation. The increase in peat in the landscape, shift to a relatively drier climate and increased temperature also explains the rapid drop in *Isoëtes* spp. at this time. Lower lake levels under a drier climate, in combination with the humic staining of lake water from the leaching of humic acids from the peat (humic stained waters are a ubiquitous feature of western Tasmanian lakes and waterways), effectively reduced the littoral habitat for *Isoëtes* spp. and expanded the habitat for moorland vegetation (see following section). Taken together, we interpret these data as indicative of a multi-millennial warming trend and low moisture between ~12.8-8.9 cal kyr BP that drove an increase in *N. cunninghamii*-dominated forest, major biomass available for burning and a decline in lake levels that facilitated blanket peat formation, with exacerbated warm and relatively drier conditions between ~11.1-8.9 cal kyr BP at the beginning of the Holocene.

Maximum expansion of *N. cunninghamii*-dominated rainforest ensued between ~8.9-5.8 cal kyr BP, featuring increases in *P. aspleniifolius* and *Eucryphia/Anodopetalum* and concurrent with declines in Blanket Moor vegetation and local biomass burning (Figs. 3 and 4), which we interpret as an increase in available moisture. A subsequent rapid decline in the *N. cunninghamii*-dominated rainforest at ~5.8 kyr led to decline in local rainforest (abundance below TPVs) and contemporaneous with an increase in buttongrass moorland (Ericaceae, *Melaleuca*; Blanket Moor) (Figs. 3 and 5) which reflects the influence of fire over a more expanded fire-prone vegetation type. In fact, these vegetational changes were coeval with a rapid increase in fire activity with a millennial-scale structure in the context of a landscape under the continued presence of people (Cosgrove, 1999), suggesting that increase in biomass burning may be attributed to human activity and ultimately modulated by climate. Hence, we interpret theses changes in fire activity as dry conditions between ~5.8-3.4 and ~1.9-0.9 cal kyr BP and wet conditions between ~3.4-1.9 cal kyr BP and the last ~900 years (Fig. 4).

A rapid increase in fire activity started during the mid-19th century (~95.0 cal kyr BP) and lasted until the present, concurrent with the appearance of exotic pants (*Rumex*, Asteraceae subfamily Cichorioideae and *Pinus*) (Figs. 3 and 4). The palynomorph *Rumex* includes native and non-native species, we think that its recent increment probably represents a major contribution from the introduced species. These changes occurred following the British invasion and conquest of Tasmania, suggesting that European occupation drove shifts in vegetation and fire activity in Tasmania. Our results are consistent with a growing body of evidence that document dramatic changes in natural environments across Australia following British invasion and highlight the potential role of Aboriginal land management in the contemporary Australian landscape (Fletcher et al., 2021b; Laming et al., 2022).

4.2. Inferences on past hydrologic changes

The palynology of Basin Lake records important changes in the abundance of the aquatic plant taxon *Isoëtes* spp. during the last ~21,000 years. *Isoëtes gunnii*, the most common member of the *Isoëtes* genus in the study region and present at the site today, inhabits shallow and clear freshwater lake environments (<1.5 m depth) in alpine and sub-alpine areas of western Tasmania (Garrett and Kantvilas, 1992). Several palynological studies have previously exploited the narrow water depth habitat range of *Isoëtes* spp. to infer shifts of shallow lake margins and ultimately monitoring changes in lake levels through time (Mariani et al., 2018; Moreno et al., 2018, 2021; Pesce and Moreno, 2014). These studies, however, report differences on the interpretation of the occurrence (lack) of *Isoëtes* spp., including the centripetal (centrifugal) shift of littoral habitats in response to a lake level lowering (rise) (Mariani et al., 2018; Moreno et al., 2021; Pesce and Moreno, 2014), and the inundation (draining) of extensive areas suitable for the growth of *Isoëtes* spp. in the periphery of the lake driven by a lake levels rise (lowering) (Moreno et al., 2018). Hence, variations in the abundance of *Isoëtes* spp. in the palynological record from Basin Lake may be open to various interpretations and using this indicator requires careful consideration of the local site morphology as it relates to the specific habitat of this taxon.

The modern morphology of the Basin Lake catchment provides a large area of <1.5 m water depth habitat for *Isoëtes* spp. on the eastern side of the lake. Flooding and draining of this large shelf in response to

lake level changes substantially alters the available habitat for *Isoëtes* spp. and, thus, we exploit this to monitor shifts in lake level from changes in the area of *Isoëtes* spp. habitat inferred from our palynostratigraphic sequence. Further, the aerial exposure of the subaqueous shelf during lowered lake levels provides habitat for terrestrial plants adapted to poorly drained regions, such as Cyperaceae species, *Melaleuca*, *Leptospermum* and other Blanket Moor buttongrass taxa. We use this as a framework to discuss the antiphase shifts in littoral macrophytes and boggy terrestrial plants to detect changes in lake level through time, with high *Isoëtes* spp. values reflecting an inundated shelf, while a high Cyperaceae, *Melaleuca* and *Leptospermum* signal a reduction of water level and colonisation by these waterlogging-tolerant species. We infer an initial phase of low lake levels at Basin Lake between ~21.0-20.0 cal kyr BP (Figs. 6 and 7) from low abundance of *Isoëtes* spp. and concurrent high Cyperaceae values and a pulse in fire (Fig. 6). This was followed by a prominent increase in lake levels that led to a maximum in *Isoëtes* spp. between ~20.0-17.7 cal kyr BP. Inferring the magnitude of lake level variation from shifts in this species is complicated by the light requirements and influence of humic acid staining of water on the depth of photic zone over the area of available habitat. Nevertheless, we infer high lake levels with low-magnitude variability (a decline at ~17.7 cal kyr BP and an increase at ~16.0 cal kyr BP) until ~12.8 cal kyr BP revealed by high *Isoëtes* spp. values and contemporaneous with a decline in Cyperaceae and relatively low biomass burning (Figs. 6 and 7). A subsequent decline in lake levels started at ~12.8 cal kyr BP and lasted until ~8.9 cal kyr BP, marked by a rapid drop in *Isoëtes* spp. and coeval with increases in *Leptospermum/Baeckea*, *Melaleuca* and fire activity (Figs. 6 and 7). We also detect a lake level rise between ~8.9-5.8 cal kyr BP, concurrent with declines in *Melaleuca* and fire activity (Figs. 6 and 7).

The correspondence in timing between our inferred lake-level changes, terrestrial vegetation and macroscopic CHAR suggests that shifts in aquatic and terrestrial ecosystems were triggered by a common driver, i.e., changes in precipitation. We posit that periods of increased precipitation led to transgressive lake-level phases that led to the inundation of extensive flatlands in the periphery of Basin Lake, thus increasing the habitat area for the establishment and expansion of *Isoëtes* spp. and reducing and/or generating a centrifugal shift of poor-drained littoral zones where species adapted to these conditions develop (Fig. 7). On the other hand, periods of reduced precipitation led to regressive lake-level phases that led to the aerial exposure and/or centripetal shift of the poor-drained littoral zone, thus enabling the expansion of species adapted to these waterlogged environments and reducing extensive inundated littoral areas where *Isoëtes* spp. can grow (Fig. 7).

We also detected lowered lake levels between ~5.8-3.4 and ~1.9-0.9 cal kyr BP given by declines in *Isoëtes* spp. that were coeval with increased fire activity (Fig. 6), and alternating with low-magnitude high lake levels between ~3.4-1.9 cal kyr BP and the last ~900 years reflected by an increase in *Isoëtes* spp. and contemporaneous with a decline in fire activity (Fig. 6). These data suggest low-magnitude oscillations in rainfall of millennial- and centennial-scale, with low precipitation between ~5.8-3.4 and ~1.9-0.9 cal kyr BP and high precipitation between ~3.4-1.9 cal kyr BP and during the last ~900 years.

4.3. Regional and hemispheric implications

Our chronology indicates that the basin of Basin Lake was ice free by at least ~21.0 cal kyr BP during the last stage of the LGM. Our reconstructed alpine grass/shrubs-dominated landscape and inferred temperature depression of at least 3.5 °C during the late LGM are consistent with previous studies from the central plateau and western Tasmania (Colhoun et al., 1999; Fletcher and Thomas, 2010b; Hopf et al., 2000). Our inference of enhanced precipitation between ~20.0-17.7 cal kyr BP, on the other hands, is in conflict with inferences of low precipitation in eastern Tasmania (McIntosh et al., 2009; Sigleo and Colhoun, 1982). Fletcher et al. (2021c) demonstrate a strong orographically derived

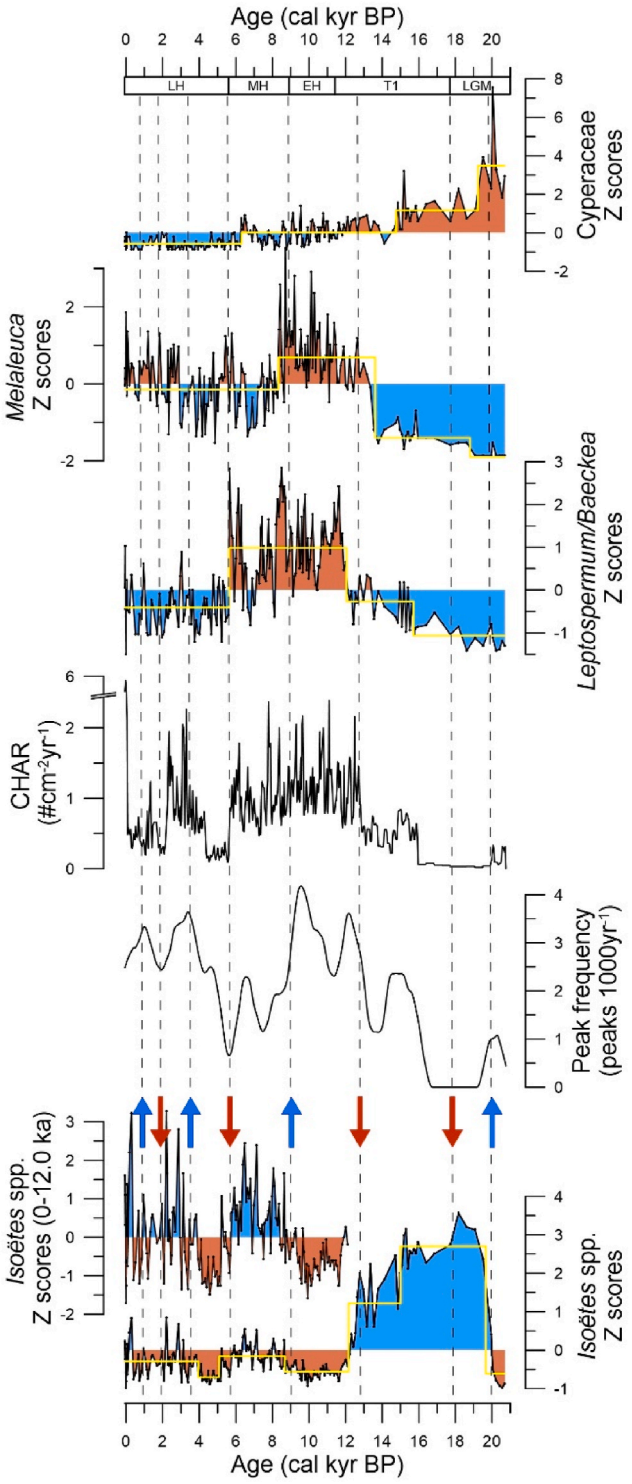

Fig. 6. Comparison of standardized abundance of *Isoëtes* spp., *Leptospermum/Baeckea*, *Melaleuca* and Cyperaceae, along with results of Change Point analyses (yellow solid lines). Also shown are the frequency and macroscopic Charcoal Accumulation Rate (CHAR). Blue areas are interpreted as high lake levels, red areas are interpreted as low lake levels. The dashed vertical lines constrain the timing of the main inferred hydroclimate changes from the Basin Lake record, accompanied with upward pointing blue arrows that indicate shifts toward wetter conditions and downward point arrows that indicate shifts toward drier conditions. The boxes below the upper X axis indicate the timing of the Last Glacial Maximum (LGM), Last Glacial Termination (T1), early Holocene (EH), middle Holocene (MH) and late Holocene (LH).

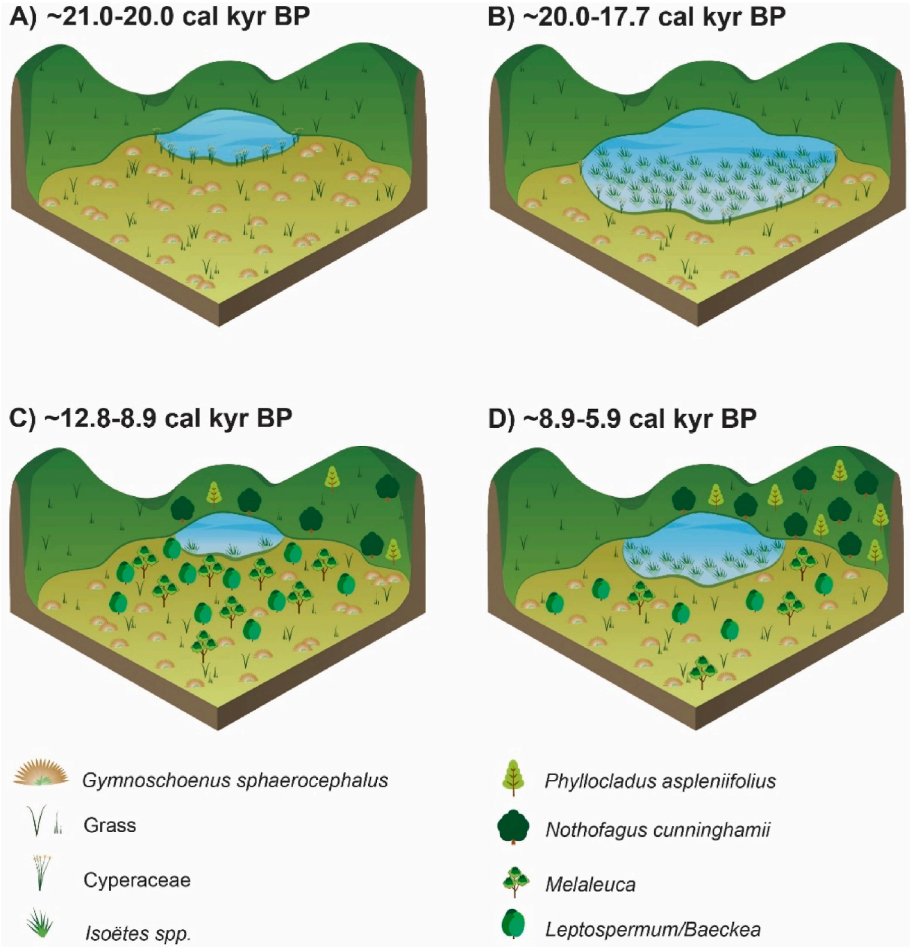

Fig. 7. Schematic representation of the main inferred lake level changes in Basin Lake. A) Low lake levels between ~21.0-20.0 cal kyr BP, B) Higher lake levels between ~20.0-17.7 cal kyr BP, C) Lake level lowering between ~12.8-8.9 cal kyr BP, and D) Lake level rise between ~8.9-5.9 cal kyr BP.

anti-phasing of moisture anomalies between west and east Tasmania in response to changes in the strength of the SWW over the island. This anti-phasing is also observed in the modern climate (Hendon et al., 2007) and therefore we suggest that a persistent SWW influence across the island between ~20.0-17.7 cal kyr BP accounts for this pattern. These changes were synchronous with mountain/cirque glacier advances elsewhere in Tasmania presumably controlled by regional changes in temperature and/or precipitation (Barrows et al., 2002; Mackintosh et al., 2006), and glacial advances and positive moisture anomalies in western Patagonia between ~40–41°S (Denton et al., 1999; Moreno et al., 1999, 2018). Collectively, these changes reflect an enhancement of SWW flow over the mid latitudes of the Southern Hemisphere that have been interpreted as a northward shift of the SWW during the LGM (Moreno et al., 1999, 2018). We posit that a northern position of the SWW reduced SWW influence on the surface of the Southern Ocean at the latitude of the Drake Passage (56°-60°S), this resulted in increased ocean stratification, reduction of upwelling in the Southern Ocean and ventilation CO_2-enriched deep water and, consequently, lowering of atmospheric CO_2 as recorded in Antarctic ice cores (Monnin et al., 2001) (Fig. 8). These results are consistent with the hypothesized role of the SWW in driving glacial-interglacial changes in the global carbon cycle (Toggweiler et al., 2006).

Increases in lowland rainforest taxa at ~17.7 cal kyr BP in the Basin Lake record mark a rapid rise in temperature during the initial stage of T1. This shift is contemporaneous with other palynological records from Tasmania and other mid-latitudes landmasses (Fletcher et al., 2021a; Moreno et al., 2015; Vandergoes et al., 2013) and with the onset of warming trends in New Zealand's South Island (Putnam et al., 2013), western Patagonia (Moreno et al., 2015) and Antarctica (Stenni et al., 2010). This trans-hemispheric correspondence suggests a tight coupling of temperature change and vegetation dynamics between mid- and high-latitudes across the Southern Hemisphere at the beginning of T1 (Fletcher et al., 2021a). In further evidence of hemispheric synchrony at this time, our inference of a lake-level decline at Basin Lake between ~17.7-16.0 cal kyr BP is contemporaneous with low lake levels reported in western Patagonia between ~42-43°S (Moreno, 2020; Moreno et al., 2018; Pesce and Moreno, 2014). This hemispheric synchrony of hydroclimatic change reflects changes in the zonal SWW at this time, with a southward shift of the moisture bearing SWW depriving the mid latitudes of moisture. A more southerly location of the SWW core at this time is also evident in the deglacial rising trend in atmospheric CO_2 revealed by Antarctic ice cores (Monnin et al., 2001) (Fig. 8), reflecting an increase in SWW wind stress over regions of the Southern Ocean at the latitude of the Drake Passage (56°-60°S) that govern changes in deep water upwelling and subsequent CO_2 ventilation to the atmosphere during the initial part of T1 (Anderson et al., 2009).

Cold-temperate conditions and increased precipitation in Basin Lake occurred between ~16.0-14.9 cal kyr BP, followed by enhanced precipitation and colder conditions between ~14.9-12.8 cal kyr BP. Our interpretation for these changes is that the SWW influence started increasing at ~16.0 cal kyr BP, followed by an intensification between ~14.9-12.8 cal kyr BP during the Antarctic Cold Reversal (ACR). Recently, Fletcher et al. (2021c) reported a compilation of pollen, charcoal and geochemical data from sites located in Tasmania to reconstruct SWW behaviour in the mid-latitudes of the Australia sector of the Southern Hemisphere spanning the ACR. These authors

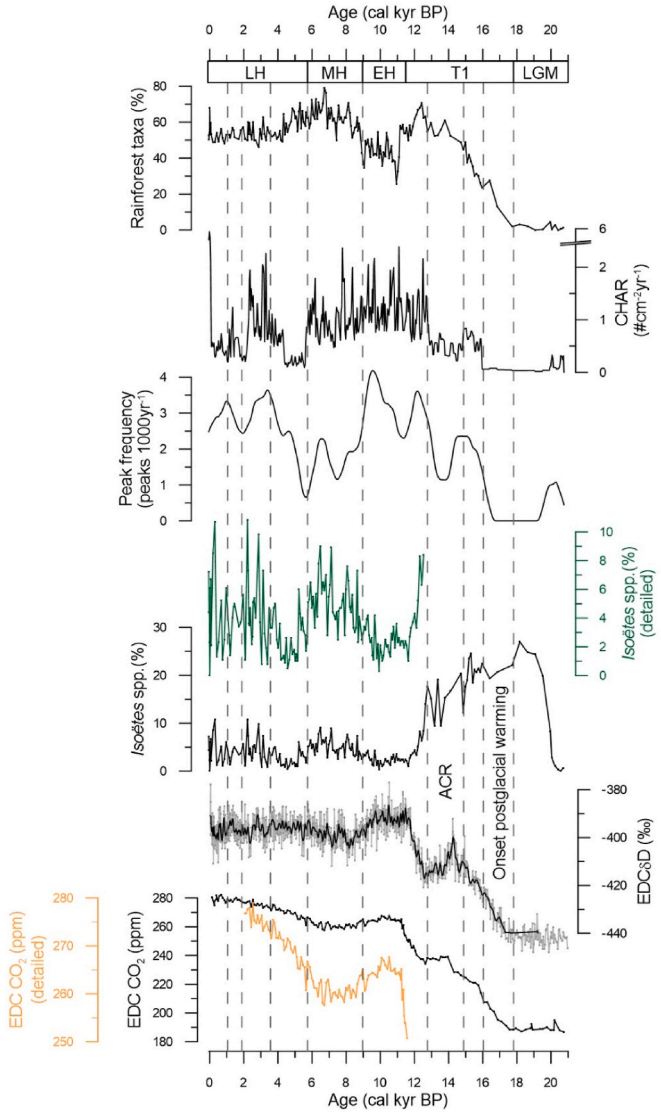

Fig. 8. Comparison of selected pollen taxa and macroscopic record from Basin Lake, along with ice data from Antarctic records (Monnin et al., 2001). The vertical dashed lines constrain the timing of the main inferred climate changes discussed in the text, indicating the onset of postglacial warming and the Antarctic Cold Reversal (ACR). The boxes below the upper X axis indicate the timing of the Last Glacial Maximum (LGM), Last Glacial Termination (T1), early Holocene (EH), middle Holocene (MH) and late Holocene (LH).

demonstrate reduced temperature and increased westerly flow over Tasmania during the ACR. The synchronicity of these trends across the Southern Hemisphere during the ACR, coupled with a reduction in Southern Ocean upwelling (Anderson et al., 2009) and a halt in the deglacial CO_2 rise (Monnin et al., 2001), reflects a norward shift of the SWW at this time (Fletcher et al., 2021c) (Fig. 8).

A multimillennial-scale rise in temperature and a decline in precipitation occurred between ~12.8-8.9 cal kyr BP, featuring diminished precipitation between ~11.1-8.9 cal kyr BP. We interpret such changes as a decline in the SWW influence starting at ~12.8 cal kyr BP which correlates with the start of a renewed Antarctic warming and resumption of the atmospheric CO_2 (Monnin et al., 2001) (Fig. 8). This was followed by reduced SWW flow between ~11.1-8.9 cal kyr BP, concurrent with peak fire activity at sub-continental and global scale (Mariani and Fletcher, 2017; Power et al., 2008; Whitlock et al., 2007) and inferred low SWW influence from other mid-latitude landmasses throughout the Southern Hemisphere (Anderson et al., 2018; McGlone et al., 2019; Moreno, 2020), suggesting a zonally symmetric decline in the strength of the SWW at the beginning of the Holocene (Fletcher and Moreno, 2012; Moreno et al., 2021). An alternative scenario involves a poleward contraction of the SWW during the early Holocene (Lamy et al., 2010), which would imply an increase in upwelling and CO_2 ventilation and rising in atmospheric CO_2 rather than the observed decrease in Antarctic ice core records (Monnin et al., 2001).

Increased precipitation levels in Basin Lake between ~8.9-5.8 cal kyr BP reduced the occurrence of fires and led to an open-canopy rainforest peak as well as an increase in lake levels (Fig. 8). These changes are consistent with maximum abundance of rainforest species (Fletcher and Moreno, 2012; Mariani et al., 2017a; Markgraf et al., 1986), a minimum in regional fire activity (Mariani and Fletcher, 2017), and an increase in moisture in western Tasmania linked to an enhancement and/or northward displacement of the SWW (Fletcher and Moreno, 2011, 2012), and contemporaneous with hydroclimatic changes throughout other Southern Hemisphere landmasses (Fletcher and Moreno, 2012).

A reduction in rainforest cover in Basin Lake since ~5.8 cal kyr BP, coupled with low-magnitude fluctuations in lake levels and fire activity reveal high climate variability characterized by alternating dry and wet periods of millennial- and centennial-scale with low precipitation between ~5.8-3.4 and ~1.9-0.9 cal kyr BP, and increased precipitation in the intervening intervals. The onset of these hydroclimate phases is synchronous with a decline in rainforest and an increase in fire activity across western Tasmania during the late-Holocene (Beck et al., 2017; Fletcher and Moreno, 2012; Mariani et al., 2017a; Rees et al., 2015; Stahle et al., 2016) and concurrent with an apparent loss of zonal SWW symmetry across the Southern Hemisphere associated with the onset of centennial and high-frequency climate variability related to ENSO and SAM-like changes (Fletcher and Moreno, 2011, 2012). These changes across the region suggest that people sought to systematically increase the area of relatively more productive open landscape by leveraging the variable climate to burn forest in favour of the comparably more resource rich moorlands in the region (Fletcher and Thomas, 2010b).

5. Conclusions

The Basin Lake record allows the reconstruction of past changes in terrestrial (vegetation and fire) and aquatic environments (lake levels) and, in turn, climate conditions from centennial to multi-millennial timescales in central-western Tasmania during the last ~21,000 years. The main conclusions are:

1. Local ice-free conditions established and persisted in the Basin Lake area at least since ~21.0 cal kyr BP. Alpine cold-resistant shrubs and herbs developed and dominated the landscape between ~21.0-17.7 cal kyr BP, along with buttongrass moorland taxa, patches of trees and relatively low fire activity. At the same time, low lake levels between ~21.0-20.0 cal kyr BP shifted to a prominent rise in lake levels between ~20.0-17.7 cal kyr BP, reflecting low and high precipitation levels, respectively. From these results we interpret cold-glacial conditions under persistent SWW influence between ~21.0-17.7 cal kyr BP, with maximum SWW influence at ~41°S over western Tasmania between ~20.0-17.7 cal kyr BP driven by a northward shift of the SWW during the final stage of the LGM.
2. The increase of rainforest taxa at ~17.7 cal kyr BP, at the expense of cold-resistant alpine herbs and shrubs and concurrent with a lake lowering reveal a warming and a decline in precipitation that mark the onset of T1. We interpret a reduction of the SWW influence related to a southward shift of the SWW at the beginning of T1.
3. The increase of arboreal cover and fire activity occurred between ~16.0-14.9 cal kyr BP, were followed by a major expansion of hygrophilous and cold-resistant species and a decline in fire activity between ~14.9-12.8 cal kyr BP. We interpret warmer/wetter conditions between ~16.0-14.9 cal kyr BP, followed by colder and enhanced precipitation between ~14.9-12.8 cal kyr BP, in response

to a rise in the strength of SWW that started at ~16.0 cal kyr BP and intensified between ~14.9-12.8 cal kyr BP.

4. A decline of rainforest, a lowering in lake level and a rise in fire activity started at ~12.8 cal kyr BP and culminated with a major openness of the landscape and enhanced fires between ~11.1-8.9 cal kyr BP. We interpret a multimillennial-scale increase in temperature and a decline in precipitation between ~12.8-8.9 cal kyr BP, with diminished precipitation between ~11.1-8.9 cal kyr BP. These results suggest a decline in SWW influence that started at ~12.8 cal kyr BP and accentuated between ~11.1-8.9 cal kyr BP at the beginning of the Holocene.
5. A sustained expansion of rainforest started at~8.9 cal kyr BP and finished at ~5.9 cal kyr BP, along with diminished fire activity and a rise in lake levels, suggesting colder and wetter conditions in response to an increase in SWW influence.
6. A shift to major openness of the landscape and variability in precipitation occurred during the last ~5800 years, with declining in precipitation between ~5.8-3.4 and ~1.9–0.9 cal kyr BP interpreted as diminished SWW influence, and rising between ~3,4-1.9 cal kyr BP and the last ~900 years, interpreted as enhanced SWW influence that allowed people to leverage climate and open the landscape with fire.
7. Rapid increase in fire activity and spread of exotic species started ~95.0 cal kyr BP, following the British invasion and conquest of Tasmania. Our results are consistent with previous studies that document dramatic changes in natural environments across Australia following post British invasion and highlight the potential role of Aboriginal land management in the contemporary Australian landscape.

Author contributions

Specific author contributions: William I. Henriquez: analysed data, conceived ideas and led writing; Michael-Shawn Fletcher: obtained the funding and sedimentary samples, contributed ideas and participated in writing and editing the manuscript; Anthony Romano: contributed ideas and participated in writing and editing the manuscript.

Declaration of competing interest

The authors declare that they have no known competing financial interests or personal relationships that could have appeared to influence the work reported in this paper.

Data availability

Data will be made available on request.

Acknowledgements

We acknowledge that our work was conducted on Tasmanian Aboriginal lands and thank the Tasmanian Aboriginal community for their support. Research was supported by Australian Research Council grants DI110100019, IN140100050 and an AINSE Award (ALNGRA12003). We thank Feli Hopf who was contracted to count the pollen. We thank Scott Nichols, Jared Pedro, Lucy Gayler and Peter Shimeld for their assistance in the field. We thank Hyebin Kim for drafting Fig. 7.

References

Adeleye, M.A., Haberle, S.G., Connor, S.E., Stevenson, J., Bowman, D.M.J.S., 2021. Indigenous fire-managed landscapes in southeast Australia during the holocene—new insights from the furneaux group islands, Bass strait. Fire 4 (2), 17. Retrieved from. https://www.mdpi.com/2571-6255/4/2/17.

Anderson, H.J., Moy, C.M., Vandergoes, M.J., Nichols, J.E., Riesselman, C.R., Van Hale, R., 2018. Southern Hemisphere westerly wind influence on southern New Zealand hydrology during the Lateglacial and Holocene. J. Quat. Sci. 33 (6), 689–701. https://doi.org/10.1002/jqs.3045.

Anderson, R.F., Ali, S., Bradtmiller, L.I., Nielsen, S.H.H., Fleisher, M.Q., Anderson, B.E., Burckle, L.H., 2009. Wind-driven upwelling in the Southern Ocean and the deglacial rise in atmospheric CO2. Science 323 (5920), 1443–1448. https://doi.org/10.1126/science.1167441.

Banks, M.R., Colhoun, E.A., Hannan, D., 1987. Early discoveries of the effects of ice action in Australia. J. Glaciol. 33 (114), 231–235.

Barrows, T.T., Stone, J.O., Fifield, L.K., Cresswell, R.G., 2002. The timing of the last glacial maximum in Australia. Quat. Sci. Rev. 21 (1), 159–173. https://doi.org/10.1016/S0277-3791(01)00109-3.

Beck, K.K., Fletcher, M.-S., Gadd, P.S., Heijnis, H., Jacobsen, G.E., 2017. An early onset of ENSO influence in the extra-tropics of the southwest Pacific inferred from a 14, 600 year high resolution multi-proxy record from Paddy's Lake, northwest Tasmania. Quat. Sci. Rev. 157, 164–175. https://doi.org/10.1016/j.quascirev.2016.12.001.

Bennett, K.D., 1996. Determination of the number of zones in a biostratigraphical sequence. New Phytol. 132 (1), 155–170. https://doi.org/10.1111/j.1469-8137.1996.tb04521.x.

Blaauw, M., Christen, J.A., 2011. Flexible paleoclimate age-depth models using an autoregressive gamma process. Bayesian Anal 6 (3), 457–474. https://doi.org/10.1214/11-BA618.

Bowman, D., Brown, M., 1986. Bushfires in Tasmania: a botanical approach to anthropological questions. Archaeol. Ocean. 21 (3), 166–171.

Bowman, D., Jackson, W., 1981. Vegetation succession in southwest Tasmania. Search 12 (10), 358–362.

Bowman, D.M., 2000. Australian Rainforests: Islands of Green in a Land of Fire. Cambridge University Press.

Chappuis, E., Lumbreras, A., Ballesteros, E., Gacia, E., 2015. Deleterious interaction of light impairment and organic matter enrichment on Isoetes lacustris (Lycopodiophyta, Isoetales). Hydrobiologia 760 (1), 145–158. https://doi.org/10.1007/s10750-015-2321-2.

Colhoun, E.A., 1985. Glaciations of the west coast range, Tasmania. Quat. Res. 24 (1), 39–59.

Colhoun, E.A., Hannan, D., Kiernan, K., 1996. Late Wisconsin Glaciation of Tasmania. and proceedings of the royal society of Tasmania. Paper presented at the Papers.

Colhoun, E.A., Pola, J.S., Barton, C.E., Heijnis, H., 1999. Late Pleistocene vegetation and climate history of lake selina, western Tasmania. Quat. Int. 57, 5–23.

Colhoun, E.A., Shimeld, P.W., 2012. Late-Quaternary Vegetation History of Tasmania from Pollen Records.

Cosgrove, R., 1999. Forty-two degrees south: the archaeology of late Pleistocene Tasmania. J. World PreHistory 13 (4), 357–402.

D'Costa, D., Kershaw, A.P., 1997. An expanded recent pollen database from south-eastern Australia and its potential for refinement of palaeoclimatic estimates. Aust. J. Bot. 45 (3), 583–605.

Denton, G.H., Anderson, R.F., Toggweiler, J.R., Edwards, R.L., Schaefer, J.M., Putnam, A. E., 2010. The last glacial termination. Science 328 (5986), 1652–1656. https://doi.org/10.1126/science.1184119.

Denton, G.H., Lowell, T.V., Heusser, C.J., Schlüchter, C., Andersen, B.G., Heusser, L.E., Moreno, P.I., Marchant, D.R., 1999. Geomorphology, stratigraphy, and radiocarbon chronology of llanquihue drift in the area of the southern lake district, seno reloncaví, and isla grande de Chiloé, Chile. Geogr. Ann. Phys. Geogr. 81 (2), 167–229. https://doi.org/10.1111/1468-0459.00057.

Faegri, K., Kaland, P.E., Krzywinski, K., 1989. Textbook of Pollen Analysis. John Wiley & Sons Ltd.

Fletcher, M.-S., Bowman, D., Whitlock, C., Mariani, M., Stahle, L., 2018. The changing role of fire in conifer-dominated temperate rainforest through the last 14,000 years. Quat. Sci. Rev. 182, 37–47.

Fletcher, M.-S., Bowman, D.M., Whitlock, C., Mariani, M., Beck, K.K., Stahle, L.N., Hopf, F., Benson, A., Hall, T., Heijnis, H., Zawadzki, A., 2021a. The influence of climatic change, fire and species invasion on a Tasmanian temperate rainforest system over the past 18,000 years. Quat. Sci. Rev. 260, 106824 https://doi.org/10.1016/j.quascirev.2021.106824.

Fletcher, M.-S., Hall, T., Alexandra, A.N., 2021b. The loss of an indigenous constructed landscape following British invasion of Australia: an insight into the deep human imprint on the Australian landscape. Ambio 50 (1), 138–149. https://doi.org/10.1007/s13280-020-01339-3.

Fletcher, M.-S., Moreno, P.I., 2011. Zonally symmetric changes in the strength and position of the Southern Westerlies drove atmospheric CO2 variations over the past 14 k.y. Geology 39 (5), 419–422. https://doi.org/10.1130/g31807.1.

Fletcher, M.-S., Moreno, P.I., 2012. Have the Southern Westerlies changed in a zonally symmetric manner over the last 14,000 years? A hemisphere-wide take on a controversial problem. Quat. Int. 253, 32–46. https://doi.org/10.1016/j.quaint.2011.04.042.

Fletcher, M.-S., Pedro, J., Hall, T., Mariani, M., Alexander, J.A., Beck, K., Blaauw, M., Hodgson, D.A., Heijnis, H., Gadd, P.S., Lise-Pronovost, A., 2021c. Northward shift of the southern westerlies during the antarctic cold reversal. Quat. Sci. Rev. 271, 107189 https://doi.org/10.1016/j.quascirev.2021.107189.

Fletcher, M.-S., Thomas, I., 2007. Modern pollen–vegetation relationships in western Tasmania, Australia. Rev. Palaeobot. Palynol. 146 (1–4), 146–168.

Fletcher, M.-S., Thomas, I., 2010a. The origin and temporal development of an ancient cultural landscape. J. Biogeogr. 37 (11), 2183–2196. Retrieved from. http://www.jstor.org/stable/40929017.

Fletcher, M.-S., Thomas, I., 2010b. A quantitative Late Quaternary temperature reconstruction from western Tasmania, Australia. Quat. Sci. Rev. 29 (17–18), 2351–2361.

Garreaud, R.D., 2007. Precipitation and circulation covariability in the extratropics. J. Clim. 20 (18), 4789–4797. https://doi.org/10.1175/jcli4257.1.
Garrett, M., Kantvilas, G., 1992. Morphology, ecology and distribution of Isoetes L. In: *Tasmania.* Paper Presented at the Papers and Proceedings of. the Royal Society of Tasmania.
Gillett, N.P., Kell, T.D., Jones, P.D., 2006. Regional climate impacts of the southern annular mode. Geophys. Res. Lett. 33 (23) https://doi.org/10.1029/2006GL027721.
Grimm, E.C., 1987. CONISS: a FORTRAN 77 program for stratigraphically constrained cluster analysis by the method of incremental sum of squares. Comput. Geosci. 13 (1), 13–35. https://doi.org/10.1016/0098-3004(87)90022-7.
Harris, S., Kitchener, A., 2005. From Forest to Fjaeldmark: Descriptions of Tasmania's Vegetation. Department of Primary Industries Water and Environment.
Hasterok, D., Halpin, J.A., Collins, A.S., Hand, M., Kreemer, C., Gard, M.G., Glorie, S., 2022. New maps of global geological provinces and tectonic plates. Earth Sci. Rev. 231, 104069 https://doi.org/10.1016/j.earscirev.2022.104069.
Hendon, H.H., Thompson, D.W., Wheeler, M.C., 2007. Australian rainfall and surface temperature variations associated with the Southern Hemisphere annular mode. J. Clim. 20 (11), 2452–2467.
Higuera, P.E., Brubaker, L.B., Anderson, P.M., Hu, F.S., Brown, T.A., 2009. Vegetation mediated the impacts of postglacial climate change on fire regimes in the south-central Brooks Range, Alaska. Ecol. Monogr. 79 (2), 201–219. https://doi.org/10.1890/07-2019.1.
Hogg, A.G., Heaton, T.J., Hua, Q., Palmer, J.G., Turney, C.S., Southon, J., Bayliss, A., Blackwell, P.G., Boswijk, G., Ramsey, C.B., 2020. SHCal20 Southern Hemisphere calibration, 0–55,000 years cal BP. Radiocarbon 62 (4), 759–778.
Hopf, F., Colhoun, E., Barton, C., 2000. Late-glacial and Holocene record of vegetation and climate from cynthia bay, lake st clair, Tasmania. J. Quat. Sci.: Publ. Quat. Res. Assoc. 15 (7), 725–732.
Ingles, A., 1985. Fire. Environmental Impact Statement into the Continuation Ofwoodchip Exportsfrom Tasmania after 1990. Retrieved from.
Jackson, W., 1968. Fire, Air, Water and Earth—An Elemental Ecology of Tasmania. Paper presented at the Proceedings of the ecological society of Australia.
Jackson, W., Bowman, D., 1982. Reply: ecological drift or fire cycles in south-west Tasmania. Search 13 (7–8), 175–176.
Jarman, S., Kantivalis, G., Brown, M., 1988. Buttongrass moorlands in Tasmania. In: Tasmanian Forest Research Council. Tasmanian Forest Research Council Research, Hobart. Report No. 3.
Juggins, S., 2016. Package "Rioja"–Analysis of Quaternary Science Data. The Comprehensive R Archive Network version 0.9-6.
Kershaw, A., Bulman, D., Busby, J., 1994. An examination of modern and pre-European settlement pollen samples from southeastern Australia—assessment of their application to quantitative reconstruction of past vegetation and climate. Rev. Palaeobot. Palynol. 82 (1–2), 83–96.
Killick, R., Eckley, I., 2014. changepoint: an R package for changepoint analysis. J. Stat. Software 58 (3), 1–19.
Kirkpatrick, J., 1982. Phytogeographical analysis of Tasmanian alpine floras. J. Biogeogr. 255–271.
Kirkpatrick, J., Dickinson, K., 1984. Vegetation of Tasmania 1: 500 000. Forestry Commission Tasmania.
Laming, A., Fletcher, M.-S., Romano, A., Mullett, R., Connor, S., Mariani, M., Maezumi, S. Y., Gadd, P.S., 2022. The curse of conservation: empirical evidence demonstrating that changes in land-use legislation drove catastrophic bushfires in southeast Australia. Fire 5 (6), 175.
Lamy, F., Kilian, R., Arz, H.W., Francois, J.-P., Kaiser, J., Prange, M., Steinke, T., 2010. Holocene changes in the position and intensity of the southern westerly wind belt. Nat. Geosci. 3 (10), 695–699. https://doi.org/10.1038/ngeo959.
Mackintosh, A.N., Barrows, T.T., Colhoun, E.A., Fifield, L.K., 2006. Exposure dating and glacial reconstruction at Mt. Field, Tasmania, Australia, identifies MIS 3 and MIS 2 glacial advances and climatic variability. J. Quat. Sci. 21 (4), 363–376. https://doi.org/10.1002/jqs.989.
Macphail, M., Hope, G., 2018. Natural Histories: an illustrated guide to fossil pollen and spores preserved in swamps and mires of the Southern Highlands. NSW. Department of Archaeology and Natural History, Research School and Pacific and Asian Studies, The Australian National University: Canberra.
Mariani, M., Beck, K.K., Fletcher, M.-S., Gell, P., Saunders, K.M., Gadd, P., Chisari, R., 2018. Biogeochemical responses to Holocene catchment-lake dynamics in the tasmanian world heritage area, Australia. J. Geophys. Res.: Biogeosciences 123 (5), 1610–1624. https://doi.org/10.1029/2017JG004136.
Mariani, M., Connor, S.E., Fletcher, M.-S., Theuerkauf, M., Kuneš, P., Jacobsen, G., Saunders, K.M., Zawadzki, A., 2017a. How old is the Tasmanian cultural landscape? A test of landscape openness using quantitative land-cover reconstructions. J. Biogeogr. 44 (10), 2410–2420. https://doi.org/10.1111/jbi.13040.
Mariani, M., Fletcher, M.-S., 2016. The Southern Annular Mode determines interannual and centennial-scale fire activity in temperate southwest Tasmania, Australia. Geophys. Res. Lett. 43 (4), 1702–1709. https://doi.org/10.1002/2016GL068082.
Mariani, M., Fletcher, M.-S., 2017. Long-term climate dynamics in the extra-tropics of the South Pacific revealed from sedimentary charcoal analysis. Quat. Sci. Rev. 173, 181–192.
Mariani, M., Fletcher, M.-S., Drysdale, R.N., Saunders, K.M., Heijnis, H., Jacobsen, G., Zawadzki, A., 2017b. Coupling of the intertropical convergence zone and southern hemisphere mid-latitude climate during the early to mid-holocene. Geology 45 (12), 1083–1086. https://doi.org/10.1130/g39705.1.
Mariani, M., Fletcher, M.S., Haberle, S., Chin, H., Zawadzki, A., Jacobsen, G., 2019. Climate change reduces resilience to fire in subalpine rainforests. Global Change Biol. 25 (6), 2030–2042.
Markgraf, V., Bradbury, J.P., Busby, J., 1986. Paleoclimates in southwestern Tasmania during the last 13,000 years. Palaios 368–380.
McGlone, M.S., Wilmshurst, J.M., Richardson, S.J., Turney, C.S.M., Wood, J.R., 2019. Temperature, wind, cloud, and the postglacial tree line history of sub-antarctic campbell island. Forests 10 (11), 998. Retrieved from. https://www.mdpi.com/1999-4907/10/11/998.
McIntosh, P.D., Price, D.M., Eberhard, R., Slee, A.J., 2009. Late Quaternary erosion events in lowland and mid-altitude Tasmania in relation to climate change and first human arrival. Quat. Sci. Rev. 28 (9), 850–872. https://doi.org/10.1016/j.quascirev.2008.12.003.
Monnin, E., Indermühle, A., Dällenbach, A., Flückiger, J., Stauffer, B., Stocker, T.F., Raynaud, D., Barnola, J.-M., 2001. Atmospheric CO2 concentrations over the last glacial termination. Science 291 (5501), 112–114. https://doi.org/10.1126/science.291.5501.112.
Moreno, P.I., 2020. Timing and structure of vegetation, fire, and climate changes on the Pacific slope of northwestern Patagonia since the last glacial termination. Quat. Sci. Rev. 238, 106328 https://doi.org/10.1016/j.quascirev.2020.106328.
Moreno, P.I., Denton, G.H., Moreno, H., Lowell, T.V., Putnam, A.E., Kaplan, M.R., 2015. Radiocarbon chronology of the last glacial maximum and its termination in northwestern Patagonia. Quat. Sci. Rev. 122, 233–249. https://doi.org/10.1016/j.quascirev.2015.05.027.
Moreno, P.I., Henríquez, W.I., Pesce, O.H., Henríquez, C.A., Fletcher, M.S., Garreaud, R. D., Villa-Martínez, R.P., 2021. An early Holocene westerly minimum in the southern mid-latitudes. Quat. Sci. Rev. 251, 106730 https://doi.org/10.1016/j.quascirev.2020.106730.
Moreno, P.I., Lowell, T.V., Jacobson Jr., G.L., Denton, G.H., 1999. Abrupt vegetation and climate changes during the last glacial maximum and last termination in the Chilean lake district: a case study from canal de La puntilla (41°S). Geogr. Ann. Phys. Geogr. 81 (2), 285–311. https://doi.org/10.1111/1468-0459.00059.
Moreno, P.I., Videla, J., Valero-Garcés, B., Alloway, B.V., Heusser, L.E., 2018. A continuous record of vegetation, fire-regime and climatic changes in northwestern Patagonia spanning the last 25,000 years. Quat. Sci. Rev. 198, 15–36. https://doi.org/10.1016/j.quascirev.2018.08.013.
Newnham, R.M., Lowe, D.J., Giles, T., Alloway, B.V., 2007. Vegetation and climate of Auckland, New Zealand, since ca. 32 000 cal. yr ago: support for an extended LGM. J. Quat. Sci. 22 (5), 517–534. https://doi.org/10.1002/jqs.1137.
Nunez, M., 1988. A Regional Lapse Rate for Tasmania. Paper Presented at the Papers and Proceedings of the Royal Society of Tasmania.
Pesce, O.H., Moreno, P.I., 2014. Vegetation, fire and climate change in central-east isla grande de Chiloé (43°S) since the last glacial maximum, northwestern Patagonia. Quat. Sci. Rev. 90, 143–157. https://doi.org/10.1016/j.quascirev.2014.02.021.
Peterson, J., Robinson, G., 1969. Trend surface mapping of cirque floor levels. Nature 222 (5188), 75–76.
Power, M.J., Marlon, J., Ortiz, N., Bartlein, P.J., Harrison, S.P., Mayle, F.E., Ballouche, A., Bradshaw, R.H.W., Carcaillet, C., Cordova, C., Mooney, S., Moreno, P. I., Prentice, I.C., Thonicke, K., Tinner, W., Whitlock, C., Zhang, Y., Zhao, Y., Ali, A.A., Anderson, R.S., Beer, R., Behling, H., Briles, C., Brown, K.J., Brunelle, A., Bush, M., Camill, P., Chu, G.Q., Clark, J., Colombaroli, D., Connor, S., Daniau, A.-L., Daniels, M., Dodson, J., Doughty, E., Edwards, M.E., Finsinger, W., Foster, D., Frechette, J., Gaillard, M.-J., Gavin, D.G., Gobet, E., Haberle, S., Hallett, D.J., Higuera, P., Hope, G., Horn, S., Inoue, J., Kaltenrieder, P., Kennedy, L., Kong, Z.C., Larsen, C., Long, C.J., Lynch, J., Lynch, E.A., McGlone, M., Meeks, S., Mensing, S., Meyer, G., Minckley, T., Mohr, J., Nelson, D.M., New, J., Newnham, R., Noti, R., Oswald, W., Pierce, J., Richard, P.J.H., Rowe, C., Sanchez Goñi, M.F., Shuman, B.N., Takahara, H., Toney, J., Turney, C., Urrego-Sanchez, D.H., Umbanhowar, C., Vandergoes, M., Vanniere, B., Vescovi, E., Walsh, M., Wang, X., Williams, N., Wilmshurst, J., Zhang, J.H., 2008. Changes in fire regimes since the Last Glacial Maximum: an assessment based on a global synthesis and analysis of charcoal data. Clim. Dynam. 30 (7), 887–907. https://doi.org/10.1007/s00382-007-0334-x.
Punt, W., Hoen, P., Blackmore, S., Nilsson, S., Le Thomas, A., 2007. Glossary of pollen and spore terminology. Rev. Palaeobot. Palynol. 143 (1–2), 1–81.
Putnam, A.E., Schaefer, J.M., Denton, G.H., Barrell, D.J.A., Birkel, S.D., Andersen, B.G., Kaplan, M.R., Finkel, R.C., Schwartz, R., Doughty, A.M., 2013. The last glacial maximum at 44°S documented by a 10Be moraine chronology at lake ohau, southern alps of New Zealand. Quat. Sci. Rev. 62, 114–141. https://doi.org/10.1016/j.quascirev.2012.10.034.
Read, J., Busby, J., 1990. Comparative responses to temperature of the major canopy species of Tasmanian cool temperate rain-forest and their ecological significance. II. Net photosynthesis and climate analysis. Aust. J. Bot. 38 (2), 185–205.
Rees, A.B.H., Cwynar, L.C., Fletcher, M.-S., 2015. Southern westerly winds submit to the ENSO regime: a multiproxy paleohydrology record from lake dobson, Tasmania. Quat. Sci. Rev. 126, 254–263. https://doi.org/10.1016/j.quascirev.2015.08.022.
Reid, J., Hill, R., Brown, M., Hovenden, M., 1999. Vegetation of Tasmania. Flora of Australia supplementary series number 8. In: University of Tasmania. CRC for Sustainable Production Forestry, Forestry Tasmania. Hobart.
Reimer, P.J., Bard, E., Bayliss, A., Beck, J.W., Blackwell, P.G., Bronk Ramsey, C., Buck, C. E., Cheng, H., Edwards, R.L., Friedrich, M., Grootes, P.M., Guilderson, T.P., Haflidason, H., Hajdas, I., Hatté, C., Heaton, T.J., Hoffmann, D.L., Hogg, A.G., Hughen, K.A., Kaiser, K.F., Kromer, B., Manning, S.W., Niu, M., Reimer, R.W., Richards, D.A., Scott, E.M., Southon, J.R., Staff, R.A., Turney, C.S.M., van der Plicht, J., 2013. IntCal13 and Marine13 radiocarbon age calibration curves 0-50,000 years cal BP. Radiocarbon 55 (4), 1869–1887. https://doi.org/10.2458/azu_js_rc.55.16947.
Riera, J.L., Ballesteros, E., Pulido, C., Chappuis, E., Gacia, E., 2017. Recovery of submersed vegetation in a high mountain oligotrophic soft-water lake over two

decades after impoundment. Hydrobiologia 794 (1), 139–151. https://doi.org/10.1007/s10750-017-3087-5.
Sigleo, W.R., Colhoun, E.A., 1982. Terrestrial dunes, man and the late quaternary environment in southern Tasmania. Palaeogeogr. Palaeoclimatol. Palaeoecol. 39 (1), 87–121. https://doi.org/10.1016/0031-0182(82)90074-8.
Stahle, L.N., Whitlock, C., Haberle, S.G., 2016. A 17,000-year-long record of vegetation and fire from cradle mountain national park, Tasmania. Front. Ecol. Evol. 4 https://doi.org/10.3389/fevo.2016.00082.
Stenni, B., Masson-Delmotte, V., Selmo, E., Oerter, H., Meyer, H., Röthlisberger, R., Jouzel, J., Cattani, O., Falourd, S., Fischer, H., 2010. The deuterium excess records of EPICA Dome C and Dronning Maud Land ice cores (East Antarctica). Quat. Sci. Rev. 29 (1–2), 146–159.
Sturman, A.P., Tapper, N.J., 1996. The Weather and Climate of Australia and New Zealand. Oxford University Press, USA.
Thomas, I., Hope, G., 1994. An example of Holocene vegetation stability from Camerons Lagoon, a near treeline site on the Central Plateau, Tasmania. Aust. J. Ecol. 19 (2), 150–158.
Thornhill, A.H., Hope, G.S., Craven, L.A., Crisp, M.D., 2012a. Pollen morphology of the myrtaceae. Part 1: tribes eucalypteae, lophostemoneae, syncarpieae, xanthostemoneae and subfamily psiloxyloideae. Aust. J. Bot. 60 (3), 165–199.
Thornhill, A.H., Hope, G.S., Craven, L.A., Crisp, M.D., 2012b. Pollen morphology of the myrtaceae. Part 2: tribes backhousieae, melaleuceae, metrosidereae, osbornieae and syzygieae. Aust. J. Bot. 60 (3), 200–224.
Thornhill, A.H., Hope, G.S., Craven, L.A., Crisp, M.D., 2012c. Pollen morphology of the myrtaceae. part 4: tribes kanieae, myrteae and tristanieae. Aust. J. Bot. 60 (3), 260–289.
Thornhill, A.H., Wilson, P.G., Drudge, J., Barrett, M.D., Hope, G.S., Craven, L.A., Crisp, M.D., 2012d. Pollen morphology of the myrtaceae. Part 3: tribes chamelaucieae, leptospermeae and lindsayomyrteae. Aust. J. Bot. 60 (3), 225–259.
Toggweiler, J.R., Russell, J.L., Carson, S.R., 2006. Midlatitude westerlies, atmospheric CO2, and climate change during the ice ages. Paleoceanography 21 (2). https://doi.org/10.1029/2005pa001154.
Vandergoes, M.J., Newnham, R.M., Denton, G.H., Blaauw, M., Barrell, D.J.A., 2013. The anatomy of Last Glacial Maximum climate variations in south Westland, New Zealand, derived from pollen records. Quat. Sci. Rev. 74, 215–229. https://doi.org/10.1016/j.quascirev.2013.04.015.
Whitlock, C., Larsen, C., 2001. Charcoal as a fire proxy. In: Smol, J.P., Birks, H.J.B., Last, W.M., Bradley, R.S., Alverson, K. (Eds.), Tracking Environmental Change Using Lake Sediments: Terrestrial, Algal, and Siliceous Indicators. Springer Netherlands, Dordrecht, pp. 75–97.
Whitlock, C., Moreno, P.I., Bartlein, P., 2007. Climatic controls of Holocene fire patterns in southern South America. Quat. Res. 68 (1), 28–36. https://doi.org/10.1016/j.yqres.2007.01.012.